Radar applications in elevator speed and location measurement

Mikko Peltola

School of Electrical Engineering

Thesis submitted for examination for the degree of Master of Science in Technology.

Espoo, 3.8.2016

Thesis supervisor:

Prof. Pekka Eskelinen

Thesis advisor:

D.Sc. (Tech.) Mikko Puranen

Aalto University
School of Electrical
Engineering

AALTO UNIVERSITY
SCHOOL OF ELECTRICAL ENGINEERING

ABSTRACT OF THE
MASTER'S THESIS

Author: Mikko Peltola

Title: Radar applications in elevator speed and location measurement

Date: 3.8.2016 Language: English Number of pages: 8+58

Department of Electrical Engineering and Automation

Professorship: Electronics and Applications

Supervisor: Prof. Pekka Eskelinen

Advisor: D.Sc. (Tech.) Mikko Puranen

Elevator speed and location measurement is traditionally implemented with motor and elevator car encoders. In this thesis, it is studied by radar. The thesis introduces the operating principles of different radars, their advantages and disadvantages. Frequency modulated continuous wave (FMCW) radars are chosen for practical tests based on these findings.

The purpose of this thesis was to evaluate the feasibility of employing radar for measuring elevator speed and location, and propose radar as the replacement of the speed and location measuring tool in the present safety system. This was studied with 24 GHz, 60 GHz and 77 GHz radars. In elevator shafts, the measurements were carried out both towards the bottom of an elevator car and a ceiling of a shaft.

The measurement results of 77 GHz radar were within the range resolution theory in all stationary cases when measured towards the ceiling. Signal attenuation degraded 60 GHz radar results at long distances. Though the results were also within the range resolution theory below 50 m distances. 24 GHz radar faced operational problems and thus accurate results were not obtained.

The ceiling of the shaft was discovered a better reflector of radar signals than the bottom of the elevator car. The elevator shaft was found out to be a suitable environment for radar measurements. Radar is a possible technology for measuring elevator speed and location, but radars tested in this thesis need further development for fulfilling the measurement criteria set by the desired application.

Keywords: Radar, FMCW, elevator, elevator shaft, frequency, bandwidth

AALTO-YLIOPISTO
SÄHKÖTEKNIIKAN KORKEAKOULU

DIPLOMITYÖN
TIIVISTELMÄ

Tekijä: Mikko Peltola

Työn nimi: Radar applications in elevator speed and location measurement

Päivämäärä: 3.8.2016 Kieli: Englanti Sivumäärä: 8+58

Sähkötekniikan ja automaation laitos

Professuuri: Elektroniikka ja sovellukset

Työn valvoja: Prof. Pekka Eskelinen

Työn ohjaaja: TkT Mikko Puranen

Hissin paikka- ja nopeusmittaus on perinteisesti toteutettu moottorin ja hissikorin enkooderien avulla. Tässä diplomityössä sitä testataan tutkalla. Työssä esitellään erilaisten tutkien toimintaperiaatteita, etuja ja haittapuolia, joiden pohjalta käytännön testeihin valittiin taajuusmoduloituja, jatkuva-aaltoisia (FMCW) tutkia.

Työn tavoitteena oli selvittää tutkan käyttökelpoisuus hissin paikan ja nopeuden mittaamiseen sekä ehdottaa sopivaa tutkaa paikka- ja nopeusmittauksen korvaajaksi nykyisessä turvajärjestelmässä. Tätä tutkittiin 24 GHz:n, 60 GHz:n ja 77 GHz:n FMCW-tutkilla, joilla mitattiin hissikuilussa sekä hissikorin pohjaa että kuilun kattoa vasten.

77 GHz:n tutka pysyi kaikissa etäisyyden mittauksien paikallaan olevissa tapauksissa etäisyysteorian erottelutarkkuuden sisällä, kun mitattiin kattoa kohti. Signaalin vaimentuminen heikensi 60 GHz:n tutkan mittaustuloksia pitkillä etäisyyksillä. Mittaustulokset olivat kuitenkin teorian rajojen sisäpuolella alle 50 metrin matkoilla. 24 GHz:n tutkalla havaittiin operatiivisia ongelmia, joiden takia tutka ei soveltunut mittauksiin.

Mittaustuloksista havaittiin, että hissikuilun katto toimii paremmin tutkasignaalien heijastimena verrattuna hissikorin pohjaan. Hissikuilu osoittautui soveltuvaksi ympäristöksi tutkamittauksille. Tutka on mahdollinen tekniikka hissin paikka- ja nopeusmittaukseen, mutta tässä diplomityössä käsitellyt tutkat vaativat parannuksia, jotta sovelluksen asettamat mittauskriteerit täyttyvät.

Avainsanat: Tutka, FMCW, hissi, hissikuilu, taajuus, kaistanleveys

Preface

KONE Oyj made this thesis possible by giving an interesting topic. I have received help from a lot of people during the thesis and I want to express my appreciation for them.

I want to thank my advisor Mikko Puranen, who was there always when I had something on my mind. Thank you for your advice and supporting to get all the things ongoing.

My supervising professor Pekka Eskelinen gave me good advice during the thesis. Also, some of the measurements were done with his equipment at Aalto University. Thank you for all the support you gave me.

I want to say special thanks to Jouni Peltonen for borrowing Elva-1 radar. It was an educational experience to build blocks for the FMCW operation of radar. I learned much.

Thank you Teemu Majasalmi and Tuomo Ropponen for manufacturing the radar corner reflector. I want to thank Jarkko Sikiö and the whole testing group in Tytyri for all the test setup supports and elevator drivings during the tests. Thank you High Rise Platforms team for the nice atmosphere. It was fun writing my thesis with you.

Finally, I want to express my gratitude to my parents and family. I appreciate much the freedom you gave me to do my own choices. Also, your endless support made my studies possible. Without that, I wouldn't be here. Last but not the least, Tiia, you deserve special thanks. You have always been there for me caring and bringing happiness to my life. I love you.

Vantaa, 3.8.2016

Mikko Peltola

Contents

Symbols and abbreviations

Symbols

a	Radar corner reflector edge length [m]
c	Speed of light in vacuum = 299 792 458 [m/s]
d_1	Fresnel zone distance of point P from one end [m]
d_2	Fresnel zone distance of point P from the other end [m]
E/N	Ratio of received energy to noise power per hertz
f	Frequency [Hz]
f_d	Doppler frequency [H]
f_p	Pulse repetition frequency [Hz]
f_s	Sampling frequency [Hz]
F	Propagation factor
F_m	The mth Fresnel zone radius [m]
G_T	Gain of the transmitting antenna in direction of the target
G_R	Gain of the receiving antenna in direction of the target
h	Height of the insulating layer [m]
k	Boltzmann's constant $\approx 1.38 \times 10^{-23}$ [J/K]
k_{tr}	Slope of the range measurement results [MHz/V]
L	Loss
m	Number of the Fresnel zone
n	Refractive index
N	Number of sampling points
P	Selectable observation point between the transmitting and receiving antenna
P_T	Transmitted power
R	Range to a target [m]
R_{max}	Maximum unambiguous range [m]
R_{min}	Minimum range [m]
R_1	Transmitting antenna distance to the target [m]
R_2	Receiving antenna distance to the target [m]
t	Time of flight [s]
t_r	Radar recovery time [s]
t_s	Time of complete frequency sweep [s]
T	Effective noise temperature [K]
w	Width of microstrip line [m]
Δf	Transmitted and received signal frequency difference [Hz]
Δf_e	Received echo signal frequency [Hz]
$\Delta f_{e,max}$	Maximum detectable echo signal frequency [Hz]
Δf_t	Transmitted signal bandwidth [Hz]
$\Delta\phi$	Phase difference
ΔR	Range resolution [m]
Δt	Delay time of target echo [s]
ϵ_r	Dielectric constant of the insulating material
λ	Wavelength [m]
σ	Equivalent reflecting area of target, radar cross section [m^2]
τ	Pulse duration [s]
τ_1	Time of observation [s]

Abbreviations

ARPANSA	Australian Radiation Protection and Nuclear Safety Agency
CW	Continuous wave
DC	Direct current
ECC	Electronic Communications Committee
ECM	Electronic countermeasure
ETSL	Emergency terminal speed limiting device
FCC	Federal Communications Committee
FFT	Fast Fourier transform
FMCW	Frequency modulated continuous wave
ICNIRP	International Commission on Non-Ionizing Radiation Protection
IF	Intermediate frequency
IRPA	International Radiation Protection Association
ISM	Industrial, scientific and medical
ITU	International Telecommunications Union
LNA	Low noise amplifier
MTI	Moving target indicator
MW	Microwave
NCRP	National Council on Radiation Protection and Measurements
PCB	Printed circuit board
RAR	Real aperture radar
RCSR	Radar cross section reduction
RF	Radio frequency
SAR	Synthetic aperture radar
SMA	SubMiniature A -connector
VSWR	Voltage standing wave ratio
WHO	World Health Organization

1 Introduction

Two functions that are essential for an elevator are the ability to recognize its speed and most importantly its location. Currently, elevators determine their speed and location by using the feedbacks of motor and car encoders. [1] For floor positioning by accuracy of ±3 millimeters, there is a reader unit connected to the bottom of an elevator car and floor code plates to walls of elevator shafts. This positioning system is illustrated in Figure 1.

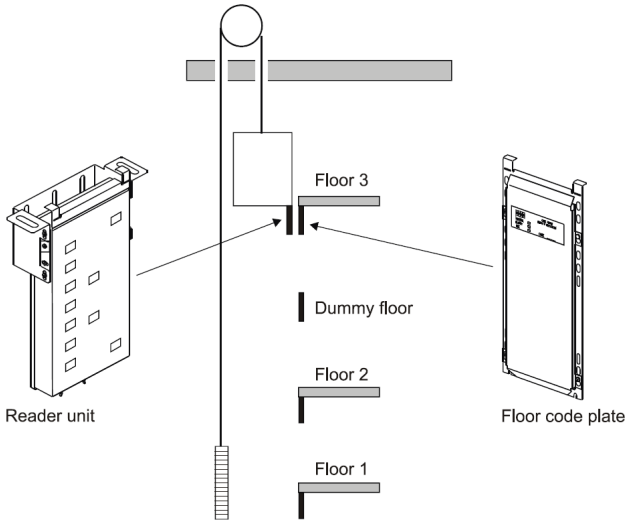

Figure 1: Locating system of a high speed elevator. [1]

This thesis focuses on high rise elevators, the speed of which exceeds 2.5 meters per second. These elevators have a safety system for preventing an elevator car running into the bottom or to the ceiling of a shaft at full speed. For that function, Emergency Terminal Speed Limiting device (ETSL) is used, which consists of several ETSL boards in a control cabinet, many switches in a shaft and two magnets on top of an elevator car. The switches on the shaft wall are connected to the control room by cables. Speed of an elevator defines the required amount of ETSL boards. For example, an elevator with a nominal speed of 4 meters per second requires two ETSL boards. These boards measure the elevator speed from the car and motor encoders in predefined shaft locations. Friction is essential for the car encoder correct operation, but safety systems cannot rely only on friction [2]. Therefore, also motor encoder speed data is used in ETSL system. When the magnets pass the ETSL switches in the shaft, the ETSL measurement is triggered. Both the car and motor encoder speed checks are triggered through independent switches. These speeds are compared and if the preset value differences are crossed, the ETSL generates an emergency stop. [1]

However, this system requires many components, which makes it expensive and laborious to install and maintain. Moreover, its data is discontinuous due to limited amount of switches in the shaft. One potential solution to overcome these issues would be using radar in ETSL system. Radars have not been used in the elevator

shafts previously, but they have been simulated with a signal generator and a network analyzer. Those results were promising.

The purpose of this thesis is to evaluate the feasibility of employing radar for measuring elevator speed and location and propose radar for the ETLS system. In order to accomplish this, the thesis compares three radar modules, which are commercially available [3–5]. However, Elva-1 [6] is borrowed for cost saving reasons. Elva-1 requires modifications and additions in order for it to function as frequency modulated continuous wave (FMCW) radar. Research will be done by testing various radar types, whose properties after a review prove to appoint the elevator application best. Tests are performed both in steel and concrete elevator shafts. In this thesis, the range goal is 300 meters and speed measurements as fast as possible although the minimum of 20 measurements per second should be obtained.

Radar is an electromagnetic device for detecting and locating reflective objects [7]. RAdio Detection and Ranging is usually shortened as RADAR. Conventional active radar transmits electromagnetic energy and receives some of the energy reflected from targets.

Radars have been widely used for numerous purposes, including detection of targets, target position and range measurement as well as angular coordinates and radial velocity, tracking and target path estimation, imaging target or area, target classification, discrimination and identification, weather observation and prediction [8, 9]. Automotive industry has become a common application for radar technology in recent years. Rear blind spot detection, reverse radar for crash warning and forward crash avoidance are typical examples of radars in new cars. Other techniques, such as ultrasonic sensors, optical sensors and cameras are also used for assisting the driver. [10] Traditional parking radar is most commonly executed with ultrasonic technology and thus it is not actually radar.

The structure of the thesis is as follows. Chapter 2 introduces current radar technologies in order to identify the most effective technology for use as an elevator speed and location measurement tool. Chapter 3 describes the radar modules based on the technology selected in Chapter 2. Chapter 4 presents the test sites, measurement arrangements and methods as well as takes a brief look into safety questions. Chapter 5 shows the measurement results for the proposed radar modules in different environments and discusses about the discoveries. Chapter 6 concludes this thesis with a brief summary as well as suggestions for further research on the topic.

2 Radar technologies

The previous chapter explained briefly what radar is and what are its common applications. Buildings are built higher and higher, which denotes that elevator shafts may exist from a couple of meters to several hundred meters. In order to find a suitable radar for elevator speed and location measurement, it is mandatory to understand different radar technologies and their special features. Therefore, this chapter introduces radar operation, types, and justifies why only some of them are chosen for further examination.

2.1 Radar targets and calibration

Electromagnetic energy travels at the velocity of light $c \approx 3 \times 10^8$ [m/s] in free space. [8] Reflections from metallic objects, refraction and diffraction may interfere with the energy propagation speed though diffraction is usually not significant in radar frequencies. Distances to the targets are measured with various techniques depending on radar types, which are presented in more detail in Section 2.2. Common ways to measure distance are a time measurement of the transmitted signal from radar to the target and back to radar and a frequency measurement of the reflected signal.

Various radars have different requirements. Mere detection, range, a constant false alarm rate, ability to discriminate different targets and operation in the presence of jamming may be the most important performance criteria for radar. For all types of radars, the ratio of received energy to noise power per hertz, E/N, is comparable. For this parameter, the basic radar equation is developed

$$\frac{E}{N} = \frac{P_T G_T G_R \lambda^2 \sigma \tau_1}{(4\pi)^3 k T {R_1}^2 F_1 {R_2}^2 F_2 L}, \tag{1}$$

where P_T is transmitted power, G_T is the gain of the transmitting antenna in the direction of the target, G_R is the received gain in the antenna, σ is the radar cross section, τ_1 is time of observation, which is determined by the time constant or allowable data rate, k is Boltzmann's constant, T is the effective noise temperature, F is a propagation factor, R_1 is distance from antenna to target, R_2 is distance from target to antenna and L is a loss factor for ohmic and similar losses. Different radar designs may be compared for the same application with the radar equation. [11]

A moving target causes a small frequency change to the reflected signal from the target. This phenomenon is called the doppler effect. The change in frequency is referred to the doppler frequency, f_d, which is calculated from the phase difference, $\Delta\phi$, [12]

$$\Delta\phi = \frac{4\pi R}{\lambda}. \tag{2}$$

The target range, R, will change due to the moving target. The target range change affects the phase difference, which is equivalent to the doppler frequency as follows

$$f_d = \frac{1}{2\pi}\frac{d\Delta\phi}{dt} = \frac{4\pi}{\lambda}\frac{1}{2\pi}\frac{dR}{dt} = \frac{2v}{\lambda}, \tag{3}$$

where v is the radial velocity of the target. It is possible to distinguish approaching and receding targets with the doppler frequency. Let the system frequency be f. Approaching targets would have a frequency of $f + f_d$ and receding ones a frequency of $f - f_d$. [12]

2.1.1 Frequency

Radars may be used in wide frequency bands from a few megahertz up to the optical and ultraviolet zone. [9] Nevertheless, most applications have been built for microwave bands between 1 and 40 GHz. The frequency of electromagnetic wave, f, is related to its wavelength, λ, by [8]

$$f = \frac{c}{\lambda}. \tag{4}$$

Used radar frequency and wavelength play a key role in radar properties. The higher the frequency is, the shorter the wavelength will be according to Equation 4. High frequency indicates better resolution for target detection due to a smaller wavelength. However, the maximum range is decreased when the frequency is raised, though, the wavelength decreased. Applications set requirements for frequencies to be used. The elevator shaft could be used as a waveguide with megahertz frequencies. Though an elevator car size sets requirements for the radar resolution. When the elevator shaft could be a waveguide, the resolution is not good enough to detect the elevator car according to Equation 4. The resolution requirement indicates suitable frequency to be found above a couple of gigahertz'.

Government regulating agencies have limited the radar signal frequency to specific frequency bands. Table 1 presents the frequency bands and the standard frequency band letter system authorized by International Telecommunications Union (ITU). These restrictions are for commercial users to guarantee other services having enough electromagnetic spectrum. Radars operating at the same frequency bands have mutual interference and for instance airplane navigation systems may not be disturbed by other devices, such as radars. [7]

Electronic Communications Committee (ECC) is responsible for developing common policies in electronic communications and harmonising the use of the electromagnetic spectrum in Europe. Federal Communications Commission (FCC) has the same function in the USA. Every country has their own agency for setting the final regulations, which is Viestintävirasto in Finland. Specific frequencies are allocated within Table 1 frequency bands. The use of the same frequency band might not be permitted all over the world. The frequency bands reserved for industrial, scientific and medical (ISM) use are freely used and therefore, using them is the easiest way to produce new applications from the licensing point of view. Table 2 presents the available frequency bandwidths concentrating on the frequencies of the radar modules that have been chosen for tests in this thesis. Frequency regulations are revised often and changes are possible. For instance, the use of 22-24.25 GHz frequency band is allowed only until 31 December 2016 in Japan [14].

Table 1: Standard radar frequency bands. [8, 9, 13]

Band designation	**Nominal frequency range**	**Spesific frequency ranges for radar based on ITU assigments for region 2**
HF	3-30 MHz	
VHF	30-300 MHz	138-144, 216-225 MHz
UHF	300-1000 MHz	420-450, 890-942 MHz
L	1-2 GHz	1215-1400 MHz
S	2-4 GHz	2300-2500, 2700-3700 MHz
C	4-8 GHz	5250-5925 MHz
X	8-12 GHz	8500-10680 MHz
K_u	12-18 GHz	13.4-14.0, 15.7-17.7 GHz
K	18-27 GHz	24.05-24.25 GHz
K_a	27-40 GHz	33.4-36.0 GHz
V	40-75 GHz	59-64 GHz
W	75-110 GHz	76-81, 92-100 GHz
mm	110-300 GHz	126-142, 144-149, 231-235, 238-248 GHz

Table 2: Available frequency bandwidths in different locations. [14–17]

	24 GHz	**60 GHz**	**77 GHz**
Europe	ISM 250 MHz (24-24.25 GHz)	ISM 500 MHz (61-61.5 GHz)	76-81GHz
USA	ISM 250 MHz (24-24.25 GHz)	59-64 GHz	76-77.5GHz, 78-81GHz
Japan	200 MHz (24.05-24.25 GHz, until 31 Dec 2016)	60-61 GHz	76-77GHz, 78-81GHz
China	ISM 250 MHz (24-24.25 GHz)	ISM 500 MHz (61-61.5 GHz)	76-77.5GHz, 78-81GHz

2.1.2 Bandwidth

Transmitted radar signal bandwidth basically represents the amount of achieved information. The larger the bandwidth is, the more information is available for target detection and separation from each other. The bandwidth of the transmitted signal is generated by widening the transmitter bandwidth by amplitude, frequency or phase modulation. Classical pulsed radars typically utilize amplitude modulation. Range resolution, ΔR, gives the minimum distance, where radars can separate two different targets. The effective signal bandwidth, Δf_t, is a significant factor determining the range resolution. For pulsed radar system, the correlation between pulse duration and the effective signal bandwidth is defined [18]

$$\Delta f_t \approx \frac{1}{\tau}. \tag{5}$$

The range resolution for pulsed radar is determined with the pulse duration, τ, [18]

$$\Delta R = \frac{c\tau}{2}. \tag{6}$$

Frequency modulation is used much in CW radars. It spreads the energy of the carrier wave over a large modulation bandwidth Δf_t. The power spectrum over the Δf_t is nearly rectangular, which helps detecting targets with high resolution. A theoretical limit for range resolution of FMCW radar is given by [18, 19]

$$\Delta R = \frac{c}{2\Delta f_t}. \tag{7}$$

Approximately, the same equation is achieved for pulsed radars by combining Equations 5 and 6. These Equations 5 - 7 imply that the higher the desired range resolution, the more signal bandwidth is needed. One meter range resolution is achieved with the bandwidth of 150 MHz, for instance.

An example of phase modulation is stepped frequency waveform, which is used both in pulsed and CW radars. The transmitted modulation bandwidth, Δf_t, is divided to equal frequency steps. After each transmitted step, the echo at a particular range is detected during the frequency sweep and the amplitude and the phase information is stored. Otherwise the phase information could not be maintained. For consecutive steps equally spaced in frequency the phase shift, $\Delta\phi$, is predicted

$$\Delta\phi = \frac{4\pi R\Delta f}{c}, \tag{8}$$

where Δf is the frequency difference of consecutive steps. This shift is apparent to doppler frequency, which is a function of range to the target. Multiple targets will each produce a unique frequency that can be extracted from the time domain signal with the Fast Fourier Transform (FFT). The range resolution to this modulation is as Equation 7, where Δf_t is the total frequency excursion of the transmitted signal. [18]

2.1.3 Environmental conditions

The operating principle of primary radar is based on reflecting electromagnetic waves from a target. Radiated energy back towards radar is dependable on target composition, size, shape and on the frequency and the nature of the carrier wave. This energy distribution is called scattering. In general, the energy is scattered in all directions. Scattering is called the radar cross section or the back scattering cross section, when the energy is scattered back towards radar. The radar cross section, σ, is not a constant and it is strongly angular-dependent of the target properties. It is represented in square meters. The higher the cross section is, the higher is the detectability. Small detectability may be an important factor for military applications. The detectability may be reduced by radar cross section reduction (RCSR), which is

achieved by shaping, with radar absorbing materials, and with passive and active cancellation. [20]

The Earth's atmosphere affects the propagation of radio waves. Generally, air is not ionized near the ground, which results in negligible small conductivity [21]. The refractive index of radio waves near the ground is between 1.00025 and 1.00040 [22]. This leads to a slight refraction of radio waves in neutral air. Attenuation of signals is significant at specific frequencies as seen in Figure 2. Especially at 60 GHz, oxygen, O_2, absorbs radiation significantly.

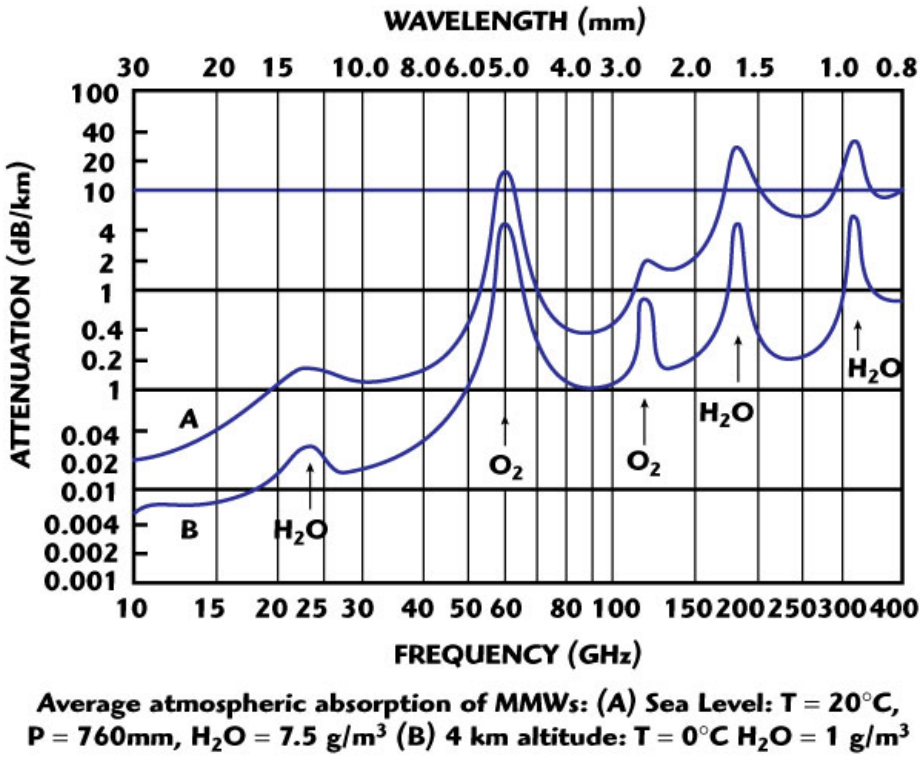

Figure 2: Average attenuation in the Earth's atmosphere. [23]

The free space propagation assumes a clear line of sight between the transmitting and the receiving antennas. Satellite communications have this situation in most occasions, but in terrestial communications obstacles like buildings, terrain or vegetation may obstruct the path. Fresnel zone equation has been provided for securing the free space propagation. Fresnel zone is an ellipsoid and its radius is as follows

$$F_m = \sqrt{\frac{m\lambda d_1 d_2}{d_1 + d_2}}, \tag{9}$$

where d_1 is the distance of the observation point P from one end, d_2 is the distance of point P from the other end and m is the number of the Fresnel zone. P is a selectable point between the transmitting and receiving antenna. The radius of Fresnel zone is at maximum at each distance when P is chosen for the middle of the transmitting and receiving antennas, in other words $d_1 = d_2$. The first Fresnel zone, $m = 1$, should

be kept free of obstructions as a general rule of thumb in order to achieve signal transmission under free space conditions. Figure 3 illustrates the first Fresnel zone in an elevator shaft. [24]

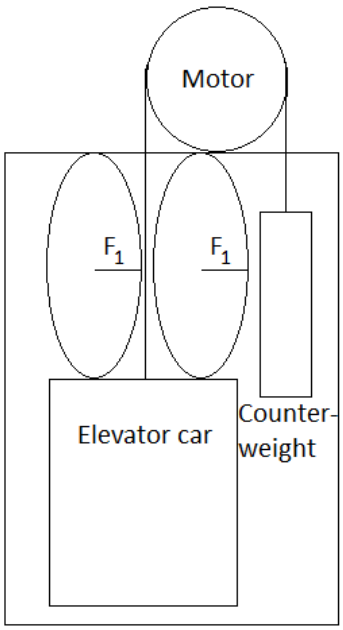

Figure 3: The first Fresnel zone illustrated in an elevator shaft on top of an elevator car.

Ropes, walls and moving counterweight are quite close to the signal path between the transmitting and receiving antennas in the elevator shaft. The radius of the first Fresnel zones at midway points, $d_1 = d_2$, at different frequencies and distances are calculated in Table 4. The smallest cross section dimensions of a high rise elevator shafts are 2.2 m * 2.3 m. The ropes are attached to the elevator car near the center of the shaft, usually around one meter from the wall. This gives the absolute maximum Fresnel zone radius of 60 cm, which is free of obstacles in the smallest shafts. Thus, in the worst case scenarios at least 300 meter ranges are achievable with the first Fresnel zone criteria fulfilled at over 60 GHz frequencies. Though the air in the shaft may be assumed as free space conditions. Nevertheless the antenna radiation pattern probably causes some reflections from walls or ropes.

The reflective properties of walls may be predicted. For that it is very important to know precisely the dielectric parameters of reinforced concrete walls for determining the transmission and reflection coefficients, which vary with the environmental conditions. [25] Steel grid square size and wall thickness are remarkable factors for reflective properties. Nevertheless, the electromagnetic field in the elevator shaft will probably be disturbed by reflections from walls, whether they are made of steel or concrete.

2.1.4 Equipment

An antenna is a device interfacing between a circuit and space. Transmitting and receiving antennas are needed in radar applications. If the same antenna transmits and receives electromagnetic energy, it is called a monostatic antenna. In bistatic radar, the transmitting and receiving antennas are separate and in different locations. Antennas are linearly, elliptically or circularly polarized. An antenna can theoretically be blind to a wave of opposite polarization. Although most of the cosmic radiation is not polarized and can be received equally well despite the antenna polarization. [26]

The most important antenna parameters are directivity, gain and the impedance match [26]. Especially the high directivity of the antenna reduces wall reflections on the application of this thesis. The elevator shaft is narrow and all reflections from walls can not be totally avoided. Thus, the amount of reflections is good to keep at minimum.

An antenna needs to be connected with radar. The connection can be done with cables or straight to the waveguide interface with a WR type connection. A typical radio frequency signal transmission cable is a coaxial cable like RG58 or RG174 [27]. One common application for coaxial cable usage is television, for example. Cable type and used frequency affect much to the signal attenuation inside the cable. Table 3 presents common cable types, their characteristic impedances and attenuations at various frequencies. Attenuation may vary with different manufacturers. Nevertheless, attenuation increases along the frequency, which makes WR type antenna connections more attractive with high frequencies.

Table 3: Coaxical cable attenuation over frequency by SSi Cable Corporation and HUBER+SUHNER. [28, 29]

		Attenuation dB/m				
Cable	Z_0 [Ω]	**1 GHz**	**10 GHz**	**20 GHz**	**60 GHz**	**77 GHz**
RG58	53.5	0.92				
RG174	50	1.12				
RG402	50	0.39	1.48	2.30		
Microbend	50	1.00	3.80	5.50	9.80	11.20

2.2 Types of radars

Radar systems may be sorted into different categories on the grounds of their special features and installation platforms. The main division between radars according to their operating principle is pulse radars and continuous wave (CW) radars. The difference between pulse and CW radar is the radiation transmission method. Pulse radars transmit repetitive pulses, whereas CW-radar transmission is continuous. Another division is primary and secondary radars, which differ from each other by propagation of signals.

2.2.1 Pulse radars

In the basic pulse radar concept, distance to the target, R, is defined with the flight time, t, of electromagnetic energy from radar to the target and back to radar. This general radar operating principle is presented in Figure 4. [8]

$$R = \frac{ct}{2}. \tag{10}$$

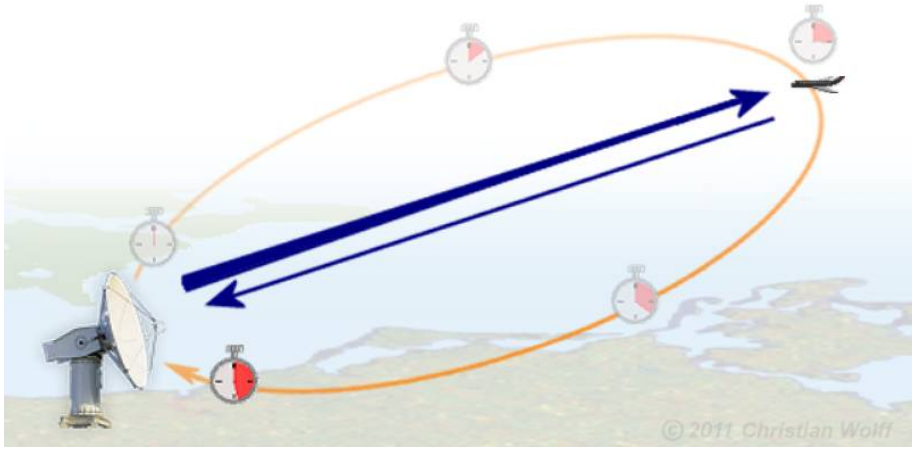

Figure 4: General pulse radar operating principle: Radar transmits energy, which backscatters from a target. Distance is calculated from the round trip time of flight. [30]

Pulse radar cannot transmit and receive pulses simultaneously, which sets limits for the minimum detectable range [31]. For a target too close, radar is still transmitting the pulse when it is already reflecting back to radar. The minimum measurable distance, R_{min}, is determined

$$R_{min} = \frac{c(\tau + t_r)}{2}, \tag{11}$$

where τ is the pulse duration and t_r is the recovery time needed for radar changing from the transmitting mode to the receiving mode. The maximum unambiguous range, R_{max}, is defined

$$R_{max} = \frac{c}{2f_p}, \tag{12}$$

where f_p is the pulse repetition frequency. [13, 31]

Moving target indication (MTI) radar is designed for detecting moving targets such as airplanes. Fixed or slow-moving unwanted targets like buildings, trees and rain are rejected at once. MTI radar utilizes the doppler shift transmitted on reflected signals. It is often called pulse doppler radar, which separates moving targets from fixed targets by comparing pulse reflection times between consecutive pulses. Reflections from a building occur exactly the same amount of time during consecutive pulses, for instance. Target motion is determined by comparing the

received signal phase with the phase of a reference oscillator in radar. The changed phases of the received signal indicate target movement. [32]

Pulse compression radar is a pulse radar, which transmits a coded pulse made by frequency or phase modulation. Bandwidth of the coded pulse is large in comparison with the uncoded pulse with the same duration. The echoed signal is processed with a pulse compression filter to decode the response from targets. The advantages of pulse compression radar are increased detection range while retaining the range resolution of radar, which uses a narrow uncoded pulse. The average power of the pulse compression radar may be increased without increasing pulse repetition frequency. Nevertheless, increasing the pulse repetition frequency decreases the unambiguous range of radar as expressed in Equation 12. [33]

In elevator application, a shaft is a closed space. Depending on the radar positioning, elevator car in the lowest or in the highest position sets the minimum range at a couple of meters. This minimum distance is too short for pulse radars to be successfully applied in the ETSL system.

2.2.2 Secondary radars

The greatest difference of primary radars to secondary radars is the two-way propagation of the signal. In primary radars, the signal has to travel to the target and back to radar, whereas one-way propagation is enough for secondary radars. General operating principle of primary radar is presented in Figure 4 and general operating principle of secondary radar is shown in Figure 5.

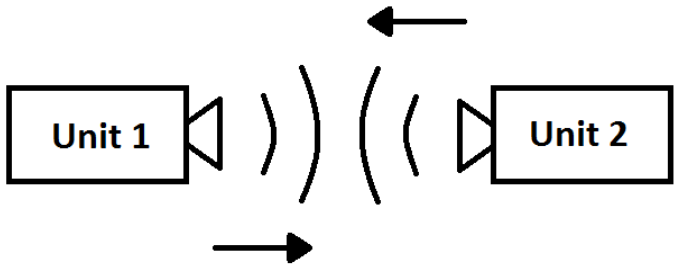

Figure 5: Secondary radar operating principle: Unit 1 transmits a signal. Unit 2 detects this signal, synchronizes it, and then transmits a similar signal back to the unit 1. Range and velocity calculations are made from the response signal in unit 1.

Secondary radar is usually referred to a radar transponder system. It has two active units, which can both operate in transmitting and responding modes. Both the CW and pulse radar techniques are possible for the radar transponder system. In the base station mode, the radar unit sends a signal. The other unit detects the signal in transponder mode. The received signal is synchronized with high precision both in time and frequency. A similar signal as the synchronized signal is then sent back to the first radar unit. Distance between units is calculated from the delay between the transmitted signal and the received response signal. The velocity is calculated from the doppler frequency shift of the response signal. For accurate

secondary radar, the high precision of synchronization is vital due to calculations are made from the response signal. [34]

Secondary radar is an interesting technology considering the ETSL system. Possibility to use various radar technologies, such as pulse and CW, in sending and receiving units make the secondary radar more customable for each application. However, the commercial availability in radar transponder systems is exiguous and thus it is not further researched in the thesis.

2.2.3 Continuous wave radars

CW radar utilizes the doppler effect and it is often referred to "doppler radar". Since CW radar transmission is continuous, the same measuring range is achieved with less power than pulse radar. Small transmission power is an asset for instance in military applications as electronic countermeasure (ECM) becomes more difficult. ECM is used for deceiving radars and tracking their locations. Though with pure CW radar only velocity measurements are possible. [31]

Typical CW radars are tracking and aperture radars. Tracking radars are aimed to receive echoes from a single target and track it in angle, in range, and/or doppler. Tracking radars usually have a narrow beam width, which makes them depended from other radars or target location information for setting the beam on the target. Tracking radar produces a high degree of precision for locating targets and prediction of their future positions. Military applications such as weapon control and missile range instrumentation are common examples of tracking radar. [35]

Radars, which first emit and then collect the radiation, are called real aperture radars (RAR). If it is desired to move the physical antenna to cover a synthetic aperture, the system is referred to synthetic aperture radar (SAR). Aircraft-mounted or satellite-mounted RAR is a typical application for SAR. SAR is mostly used for airborne or spaceborne ground mapping. Signal processing of the SAR radar system is also complicated and it requires much computing performance. [36]

Range information from CW radar is achieved by modulating the frequency of the continuous radar signal. This type of radar is called frequency modulated continuous wave (FMCW) radar. FMCW radars have many advantages. First of all, frequency modulation is compatible with wide variety of solid-state transmitters. Linear frequency modulation is the most versatile, but sinusoidal modulation has also been used in the past. Second, the frequency measurement can be done with digital processors using FFT, which makes the signal processing easier. Third, FMCW radar signals are difficult to detect with conventional intercept receivers. [37]

The operating principle of FMCW radar is presented in Figure 6. The transmitted signal is presented with green and the received signal with red. The received signal is delayed the amount of

$$\Delta t = \frac{2R}{c'}, \tag{13}$$

where refractive index, n, is taken into account by

$$c' = \frac{c}{n}. \tag{14}$$

Frequency difference is constant between the transmitted and the received signal if the power of the transmitter is linearly frequency modulated. Delay time of target echo signal, Δt, is found out from the frequency differences

$$\Delta f_e = \frac{\Delta t \Delta f_t}{t_s}, \tag{15}$$

where t_s is the time of the complete frequency sweep, Δf_e is the frequency of the echo signal and Δf_t is the bandwidth of the radar frequency sweeps. Equations 14 and 15 are rearranged to Equation 13 in order to get the target range, R [38]

$$R = \frac{c' \Delta t}{2} = \frac{c \Delta f_e t_s}{2 n \Delta f_t}. \tag{16}$$

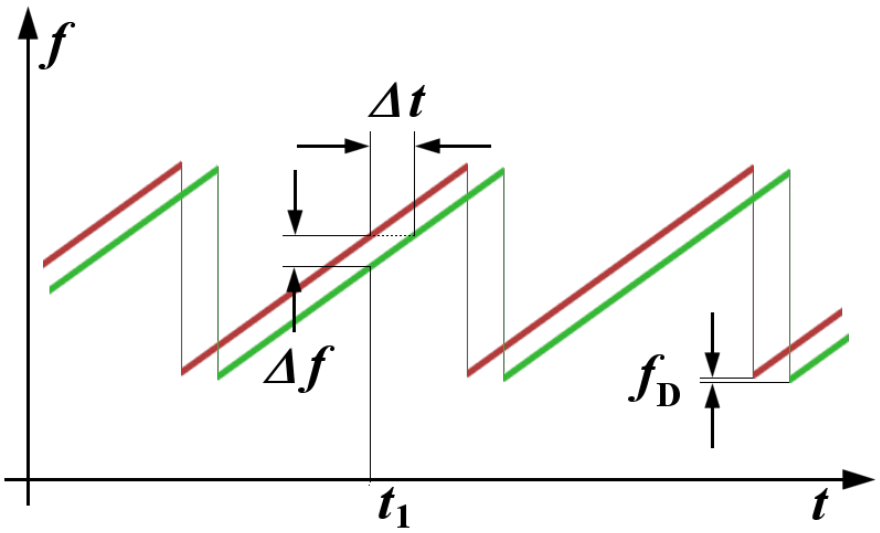

Figure 6: FMCW radar operating principle. The time delay, Δt, is proportional to the frequency difference, Δf, of transmitted and received signal if the Doppler frequency, f_D, may be ignored and the transmitter's power is linearly frequency modulated. [39]

The range information acquired by Equation 16 has an upper threshold. The sampling criteria of Nyqvist has to be fulfilled for unambigious range information. The sampling frequency of signal, f_s, is achieved by

$$f_s = \frac{N}{t_s}, \tag{17}$$

where N is the number of sampling points. The highest unambiguous range is calculated with the maximum detectable echo frequency $\Delta f_{e,max}$. Fulfilling Nyqvist sampling criteria $\Delta f_{e,max}$ is given by

$$\Delta f_{e,max} = \frac{f_s}{2}. \tag{18}$$

Setting this frequency to Equation 16 the maximum unambiguous range, R_{max}, is defined by

$$R_{max} = \frac{\Delta f_{e,max} t_s c}{2n\Delta f_t} = \frac{Nc}{4n\Delta f_t}. \tag{19}$$

Equation 19 shows that the maximum range can be expanded by increasing the sampling points or decreasing the transmitted signal bandwidth. [18]

Continuous wave radar technologies generate much interest considering the ETSL system. Properties of FMCW technique look promising and FMCW radars are commercially available. A carrier wave frequency of FMCW radar does not affect the accuracy of radar, but it probably affects the radar behavior in an elevator shaft and thus, several frequencies are to be tested. The chosen FMCW radar modules for tests are 24 GHz by Infineon Technologies, 60 GHz Elva-1 and 77 GHz by Sivers IMA.

2.3 Radar corner reflector

Radar corner reflectors have a high back scattering radar cross section over a wide angular range. [40] They do not require any power to operate, are mechanically easy to manufacture, and operation in difficult conditions is not a problem. In elevator application, the influence of a radar corner reflector is studied. It provides better back scattering conditions than the elevator car or the elevator shaft ceiling. A radar corner reflector generates a radar cross section according to Equation 20

$$\sigma = \frac{4\pi a^4}{3\lambda^2}, \tag{20}$$

where a is the dimension of the inner edge of the corner reflector [41, 42]. Table 4 presents the radar cross section areas calculated by Equation 20 of the chosen radar modules.

Table 4: Radar signal wavelengths, the cross section areas and the first radius' of the Fresnel zones at different distances and frequencies are calculated by Equations 4, 9 and 20. Edge length of the corner reflector is 15 cm.

	24 GHz	**60 GHz**	**77 GHz**
λ [cm]	1.25	0.50	0.39
σ $[m^2]$	13.59	84.94	139.89
$d_1 + d_2 = 50m, F_{m=1}$ [m]	0.40	0.25	0.22
$d_1 + d_2 = 300m, F_{m=1}$ [m]	0.97	0.61	0.54
$d_1 + d_2 = 500m, F_{m=1}$ [m]	1.25	0.79	0.70

Reflectors made of three mutually orthogonal metal plates will have the most of the incoming rays reflecting three times, as long as the reflector dimensions are greater than three wavelengths [43]. Three reflections are a must for a signal to

turn around 180 degrees parallel back towards the radar. The most practical corner reflectors have dimensions ten times wavelength [41]. In this thesis, 24 GHz, 60 GHz and 77 GHz primary radars are tested with the corner reflector. Wavelengths of the signals are calculated at these frequencies in Table 4. Though, less than 5 centimeter edge length would be the optimized size of the corner reflector, but in the elevator shaft space is not the limiting factor. For practical reasons, the radar reflector edge length, a, was chosen for 15 cm. The dimension also exceeds ten wavelengths in all radars under testing. The manufactured radar corner reflector is presented in Figure 7. Base material is two millimeter thick zinc coated metal sheet. Aluminum tape is used to cover the junction holes.

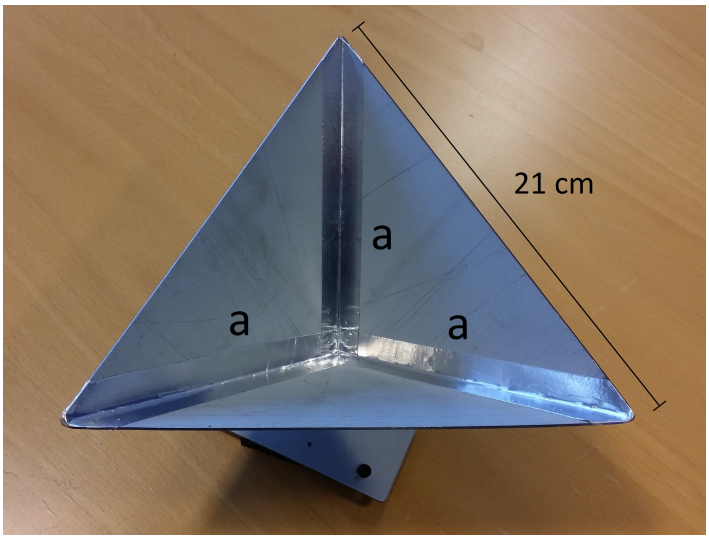

Figure 7: Radar corner reflector with dimensions $a = 15$ cm.

All surfaces with surface roughness « 0.1 λ rms are smooth and conduct perfectly. [44] The resistance of metals at microwave frequencies is increased by skin effect though the resistive loss usually remains negligible and metal surfaces form good mirrors at centimetric wavelengths. Aluminum and copper would be slightly better materials for the reflector though they are expensive compared with zinc. In addition, zinc is very effective in protecting steel against corrosion and thus it has been chosen for the material of the radar corner reflector [45].

3 Radar modules

Chapter 3 presents the radar modules chosen for tests in Chapter 2. The radar modules to be described are all FMWC radars, which are 24 GHz of Infineon Technologies, 60 GHz Elva-1 Front-End radar and 77 GHz of Sivers IMA.

3.1 Infineon Technologies 24 GHz

Sense2Go2 development kit of Infineon Technologies consists of a 24 GHz radar chip (BGT24MRT11) and a microcontroller (XMC4200). Only a microUSB connection to a pc is required for correct operation. Radar operative blocks are seen in the block diagram of Figure 8.

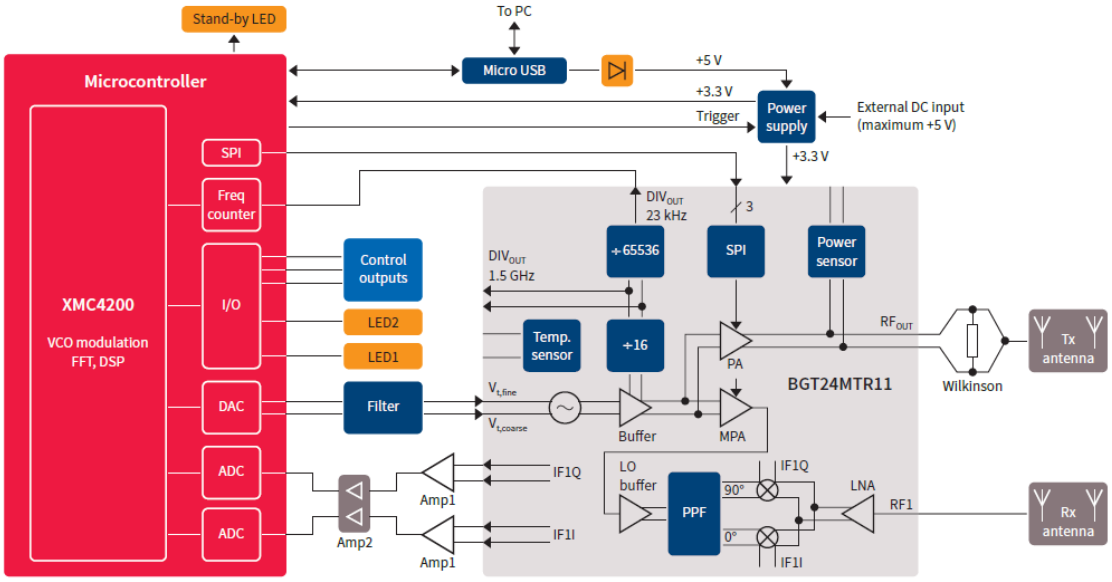

Figure 8: Sense2Go2 block diagram. [3]

The radar chip has two integrated antennas. To get better antenna directivity and performance, the chip is remodeled to get Flann Microwave's 20880-PA-3514 lens horn antennas of Figure 10 connected. The antenna lens diameter is 274 millimeters and nominal mid band gain is 34 dBi.

Microstrip lines on top of insulating materials are commonly used waveguides in microwave technology. [46] H. A. Wheeler has derived equation

$$Z_c = \frac{42.5\Omega}{\sqrt{\epsilon_r + 1}} ln[1 + \frac{4h}{w}(\frac{4h}{w}\frac{14\epsilon_r + 8}{11\epsilon_r} + \sqrt{(\frac{4h}{w})^2(\frac{14\epsilon_r + 8}{11\epsilon_r})^2 + \frac{\epsilon_r + 1}{2\epsilon_r}\pi^2})] \quad (21)$$

for the characteristic impedance of microstrip lines, where h is the height of the insulating layer, w is the width of the microstrip line, and ϵ_r is dielectric constant of the insulating substance. Due to remodeled radar chip, impedance matching is confirmed by calculating the new impedance by Equation 21. According to the data

sheet of the radar module, $h = 0.254$ [mm] and dielectric constant of substance $RO4350B$ is $\epsilon_r = 3.48 \pm 0.05$. Width, w, is 0.5 [mm], which is read about Figure 9 by Gerberlogix software. With these dimensions, Z_c is between 54.17 Ω and 54.85 Ω.

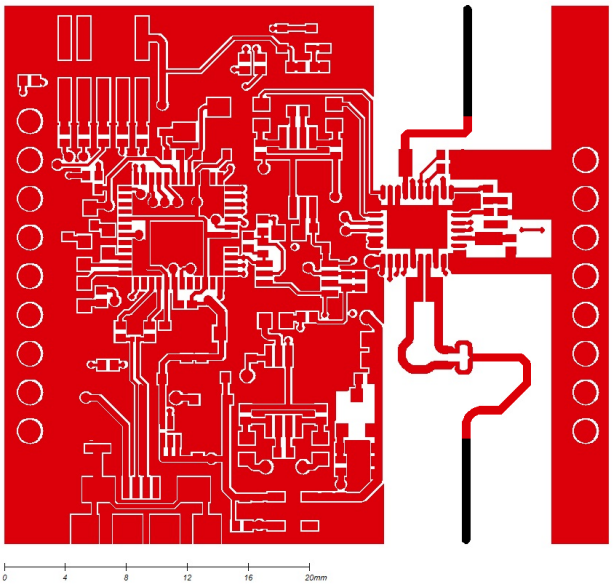

Figure 9: Sense2Go2 modified printed circuit board (PCB). Added antenna traces are highlighted with black. Transmitting antenna trace is lower and receiving antenna trace is upper.

SubMiniature A (SMA) connectors are cheap and their availability is good. SMA connectors operate mode-free up to 18 GHz and some versions up to 27 GHz, whereas 2.92 mm connectors operate up to 40 GHz [47]. SMA and 2.92 mm connectors are mechanically mateable, but the electrical performance at the connector interface need to be considered as well. Paul Pino [48] presents SMA to 2.92 mm connection impedances. Impedance through interface transition in the optimal gap is 50.1 Ω and impedance variation over the range of gaps is measured to be 0.2 Ω. [48] Voltage standing wave ratio (VSWR) 1.054:1 in SMA to 2.92 mm connection is never exceeded.

Antennas of Flann Microwave of Figure 10 have 2.92 mm connectors. Although electrical differences in SMA to 2.92 mm connection are noted, no significant changes in electrical properties are found [48]. Hence, 2.92 mm to SMA connector mateability, a low price of the SMA and good availability, SMA connectors are connected to the modified Sense2Go2 PCB. Two semirigid RG402 coaxial cables with the length of 55 cm are used for connecting the antenna to the radar chip. These cables have SMA connectors.

Infineon Technologies provides software with the development kit. The radar module can be used and controlled with this software. It also calculates the distance to the target.

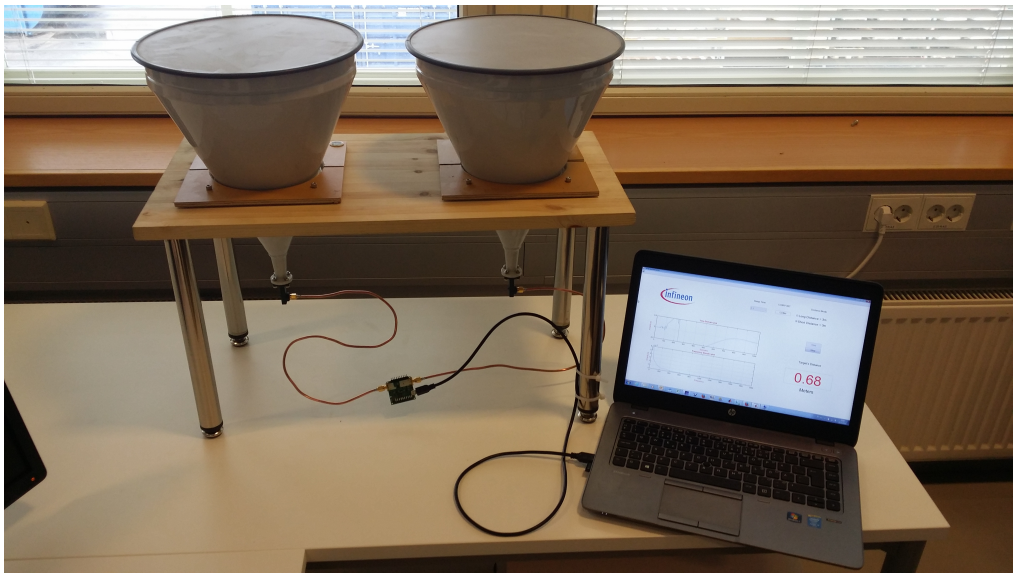

Figure 10: Antennas attached to the 24 GHz radar module by RG402 cables.

3.2 Elva-1 60 GHz

Elva-1 Front-End radar is 60 GHz radar, whose simplified block diagram is presented in Figure 11. A radar signal is produced from the base frequency of 7.256 GHz. Sample is taken to the receiver through a 1:5 power divider and after that the base frequency is multiplied with factor 8. This 58.048 GHz signal is mixed with a modulated intermediate frequency (IF) to produce the actual waveform. The antenna of the radar is a parabolic reflector with a Cassegrain-type feed. This antenna type includes the transition from WR-15 waveguide to a circular horn. Side lobes are suppressed with the equipped cylindrical collar. The received radar signal is down converted to the intermediate frequency using the sampled 7.256 GHz frequency as a local. [6]

A correct operation of radar is checked with the measurement setup of the block diagram presented in Figure 12. The measurement equipment are shown in Figure 13. A DC power supply OF1731SL, Rohde & Schwartz's DC power supply NGPV 20/10, signal generator 8683D and spectrum analyzer 8563A of Hewlett Packard are used in the setup. Two meter RG-58 cables are used for connecting the IF signal generator and the spectrum analyzer to Elva-1. The signal generator supplies an IF frequency of 2.48 GHz with a 0 dBm level and a peak of -12.33 dBm is detected with the spectrum analyzer from the radar receiver.

A saturation point is searched by keeping the IF frequency of 2.4943 GHz constant and then observing the spectrum analyzer while changing the signal generator power level. Table 5 presents the measured points. Results show that the saturation point is near 6 dBm. After that the power level is put back to 3 dBm and then the signal generator is connected straight to the spectrum analyzer. This power peak is 0.17 dBm.

Elva-1 needs additional components to be able to operate as FMCW radar. IF

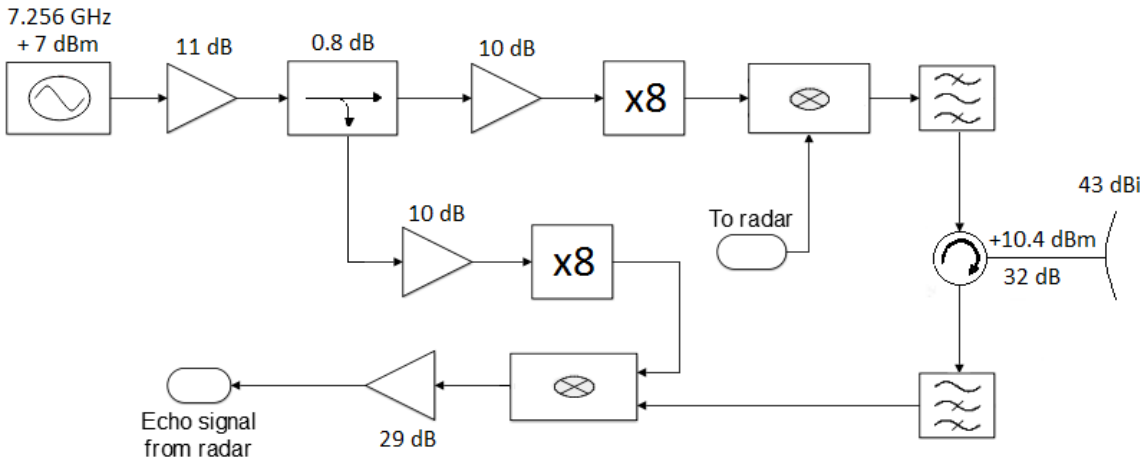

Figure 11: A block diagram of the Elva-1 front-end radar. [6]

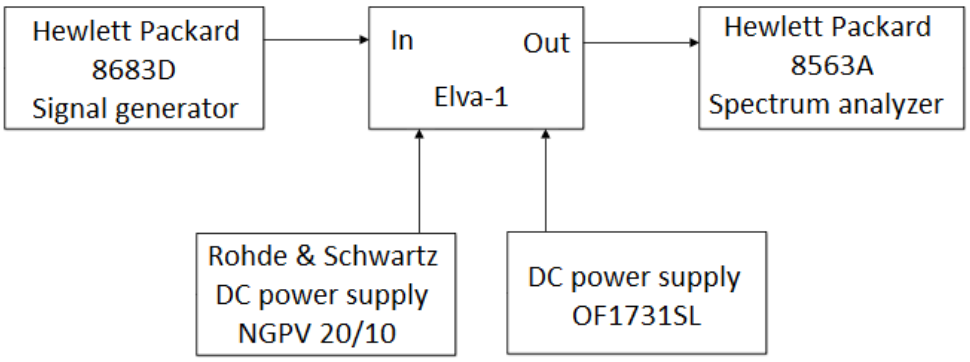

Figure 12: A block diagram of the measurement setup.

signal to radar and echo signal processing units of Figure 11 have to be built. A block diagram of the built signal processing components is presented in Figure 14.

The frequency of 2.45 GHz is provided for the radar mixer by a voltage controlled oscillator. The oscillator is fed by a signal generator of Agilent series 33500B,

Table 5: Elva-1 radar saturation point.

Signal generator level	**Measured radar peak level**
0 dBm	-11.05 dBm
3 dBm	-8.07 dBm
6 dBm	-5.22 dBm
3 dBm	-7.82 dBm

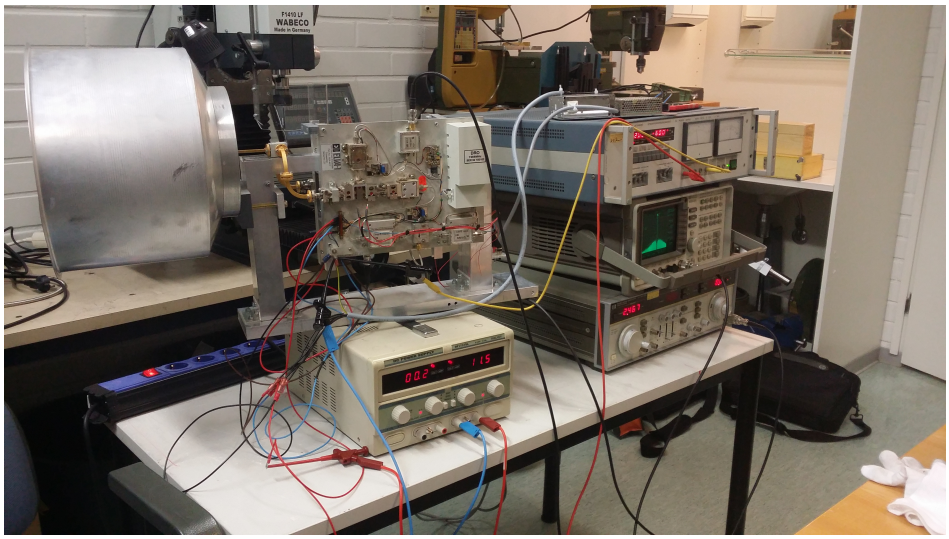

Figure 13: Testing Elva-1 front-end radar

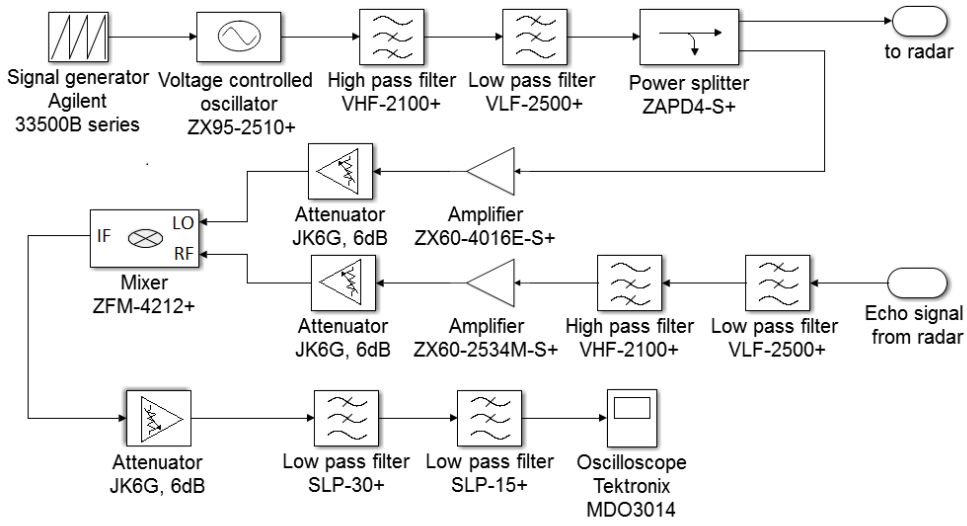

Figure 14: A block diagram of the signal processing components for FMCW radar operation.

which produces a sawtooth waveform. That provides maximum bandwidth in linear adjustment range. The frequency of the oscillator is determined by measuring its output frequency with different tuning voltages. Oscillator tuning voltage area is up to five volts and its output frequency is measured with the tuning voltage intervals of 0.5 volts. Results are shown in Figure 15. A slope is found in the results to be 92.36 MHz/V. The signal generator is feeding the oscillator with a peak to peak amplitude of two volts. The actual output voltage of the signal generator is checked with an oscilloscope and found to be 4.08 volts. This voltage sets the frequency variation of the oscillator at 376.81 MHz, which is the transmitted signal bandwidth, Δf_t, in

Equation 16. With this bandwidth, the range resolution is 40 cm by Equation 7 and the maximum range is 300 m by Equation 19.

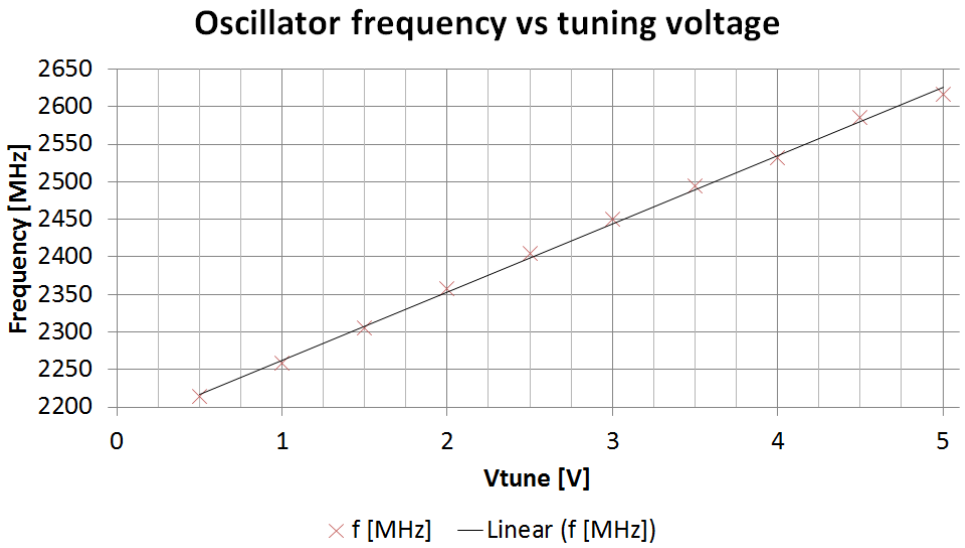

Figure 15: Measurement results of the oscillator frequency at different tuning voltages.

The unwanted harmonics of the signal are filtered with low and high pass filters right after the voltage controlled oscillator. A power divider splits the signal to radar and forwards a sample of an original signal to a mixer for echo analysis. The mixer requires a local oscillator signal with high power, hence an amplifier is put between the power divider and the mixer. An echo signal from the target is first filtered with low and high pass filters. Then the echo signal is amplified before heading to the mixer. There is one six dB attenuator after both amplifiers before the mixer and one attenuator after the mixer. The signal is filtered with two low pass filters after the mixer and this echo signal, Δf_e, is measured with an oscilloscope. Time of complete frequency sweep, t_s, is calculated from the signal generator frequency by

$$t_s = \frac{1}{f}, \tag{22}$$

where f is the signal generator frequency. A refractive index, n, for air is assumed as 1.0003 [22]. Distance to the target can be calculated by Equation 16.

The practical layout for signal processing components is shown in Figure 16. These components are attached to a metal plate for a good ground connection. The specific data of the components are found in Table 6. The components are ordered from manufacturer Mini-Circuits. External power supplies are used for powering the system. A voltage regulator is fed with + 12 volts, which makes + 5 volts for the oscillator and the ZX-60-2534M-S+ amplifier. The other amplifier, ZX60-4016E-S+, requires + 12 volts, which is produced by an external power supply.

Table 6: Specific data of the signal processing components.

Component	Function	Frequency
ZX60-2534M+	Amplifier	0.5 - 2.5 GHz
ZX60-4016E-S+	Amplifier	0.02 - 4.0 GHz
JK6G	Attenuator 6 dB	
VHF-2100+	High pass filter	2.2 - 6.0 GHz
VLF-2500+	Low pass filter	DC - 2.5 GHz
SLP-30+	Low pass filter	DC - 32 MHz
SLP-15+	Low pass filter	DC - 15 MHz
ZFM-4212+	Mixer	2.0 - 4.2 GHz
ZAPD-4+	Power splitter	2.0 - 4.2 GHz
ZX95-2510+	Voltage controlled oscillator	2.3 - 2.51 GHz

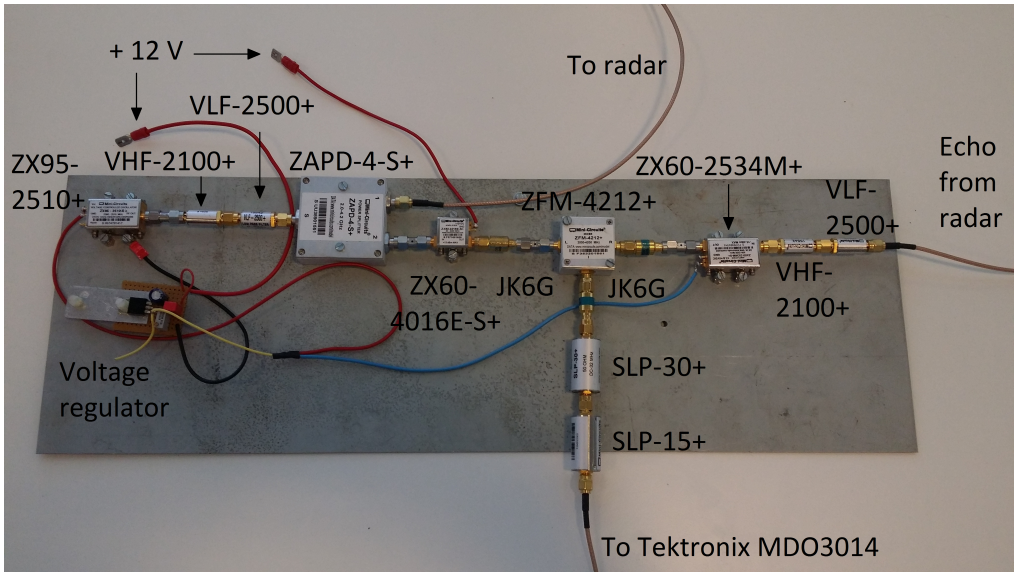

Figure 16: Signal processing components on a metal plate. A voltage regulator is on the left below the voltage controlled oscillator. Signal goes to the radar from power divider port 1 and comes back through the filters by the right side. The echo frequency is measured with oscilloscope below the mixer.

3.3 Sivers IMA 77 GHz

Sivers IMA RS3400W/04 is a complete W-band FMCW front end radar module. It has synthesized frequency source and a wideband sweep, Δf_t, of 1.5 GHz. According to Equation 7, a 10 cm range resolution is achieved with this transmitted signal bandwidth, which is the maximum resolution of this module. Sivers IMA has a power controller board CO1000A/00, which provides biasing and a pc interface to the system. The controller board is connected to a pc with RS232-communication. Radar module frequency sweep control and measured radar signal data is achieved over

the serial connection. The radar module is fed with +5.5 volts and power controller board with + 12 volts by external supplies. The operative blocks of the module are seen in the diagram of Figure 17.

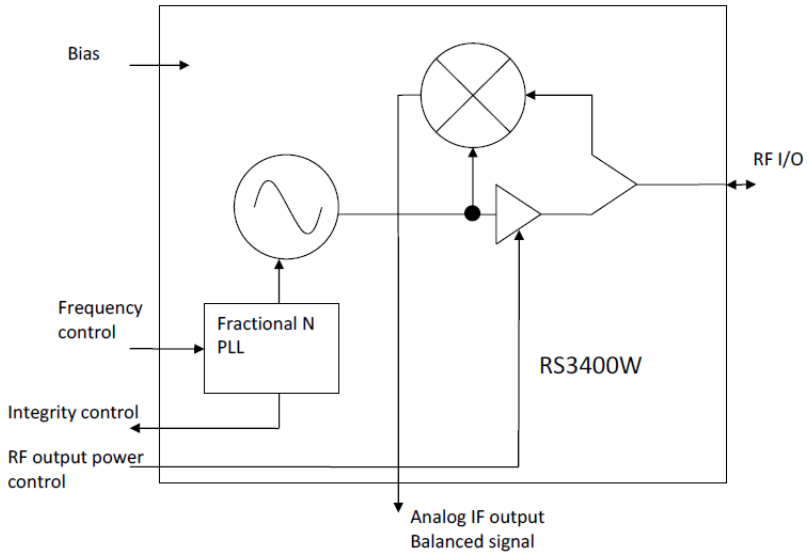

Figure 17: Block diagram of RS3400W/04. [4]

Sivers IMA's radar sensor is connected to a high directivity antenna by a WR12 waveguide interface. Lens horn antenna 26880-TA-9498 of Flann Microwave is used in the tests with this radar module. Diameter of the lens is 100 millimetres and the nominal mid band gain is 37 dBi. The radar module, the power controller board and the antenna connections are presented in Figure 18.

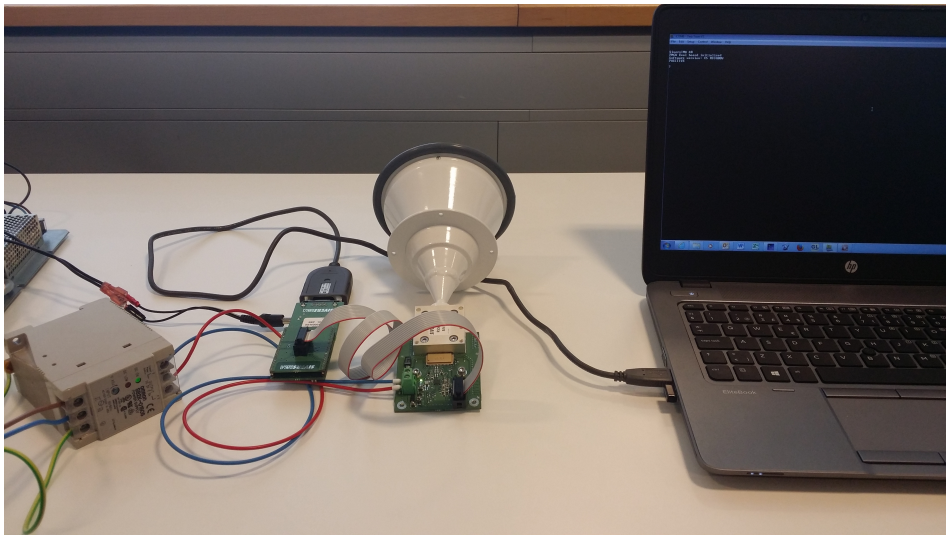

Figure 18: Radar module and antenna connected to the power controller board, which is connected to a pc with RS232-communication. The radar module is fed with +5.5 V and the power controller board with +12 V by external power supplies.

RS3400W/04 is a synthesized module, which sweeps the frequency in steps with a set of discrete frequency points. The output of the sensor corresponds to the cosine of the phase difference between the transmitted and received signals. This cosine signal indicates the round-trip electrical distance, which the transmitted signal has travelled. During a frequency sweep, the phase change of the received signal compared with the transmitted signal has to be estimated to get the distance to a target. One way to do it is to take the Fourier transform of the signal. [49]

Configuration of radar is done with a terminal program over the serial connection. RS3400W/04 is set to perform one frequency sweep, which lasts 75 ms. Sampling points, N, are set at maximum, which is 1501. Measuring takes 50 microseconds at each point. The module returns the sampled raw data points of the sweep. FFT is calculated with Matlab software to get the radar echo frequency, Δf_e, from a reflective surface. The target range information is acquired by Equation 16.

4 Measurements

This chapter presents the general measurement arrangements and the test sites in Hyvinkää and Lohja. Safety questions are considered in the end of the chapter.

4.1 Measurement arrangements

With each radar, the first measurements are made towards the sky, in other words, there are no obstacles producing reflections. This simulates the situation of free space propagation, which is an important result when comparing with the results of elevator shafts. In an elevator shaft, the first measurements are made when an elevator car is stopped at each measurement point to get better understanding about the radar properties in the elevator shaft.

Two different practical test setups are possible and both of them are tested. In the first case, radar, antennas and other measuring devices are at a bottom of an elevator shaft and measuring is made towards a bottom of an elevator car. In the second case, the measuring devices are on top of an elevator car and measuring is made towards a ceiling of an elevator shaft. Effect of the Figure 7 radar corner reflector is tested in each case with every radar. The corner reflector is attached to the bottom of the elevator car with magnets or to the ceiling of the shaft.

In Hyvinkää, antennas are placed at the center between the ropes and the counterweight. With this placement, the possible disturbing effects of the moving counterweight should occur if they exist when measuring towards the bottom of the car. On top of the elevator car, radar is more practical to attach between the ropes and the side wall across the counterweight. This placing is as far from the counterweight as practically possible. Antennas are also connected closer to elevator car corner for securing the first Fresnel zone free of obstacles. These placements are illustrated in Figure 19 and the photos of both situations are presented in Figures 20 and 21.

Power to the elevator car is transferred with travelling cables. The higher the elevator shaft is, the longer these moving elevator cables are. In Tytyri, the cables move at the center between the door side wall and ropes and would probably disturb the measurements from the center of the door side wall and ropes. Therefore different placement is tested in measurements in Tytyri for knowledge of possible counterweight effects.

At the bottom of the shaft in Tytyri, antennas are placed at the center between the ropes and the back side wall. This placement is the worst case scenario if the counterweight has disturbing effects. Though the first Fresnel zone is clear of obstacles with this placement. On top of the elevator car, radar is placed on the other side of ropes for practical reasons. On top of the car inside the spoiler, the door side half has much more space than the backside. These placements are illustrated in Figure 22. Photos of the measurement setups towards the bottom of the elevator car are seen in Figures 23 and 24. A 50 centimeter hole is left on an air drag reduction spoiler for radar signal transmission. This hole and photos of the measurement setups on top of the elevator car are seen in Figure 25.

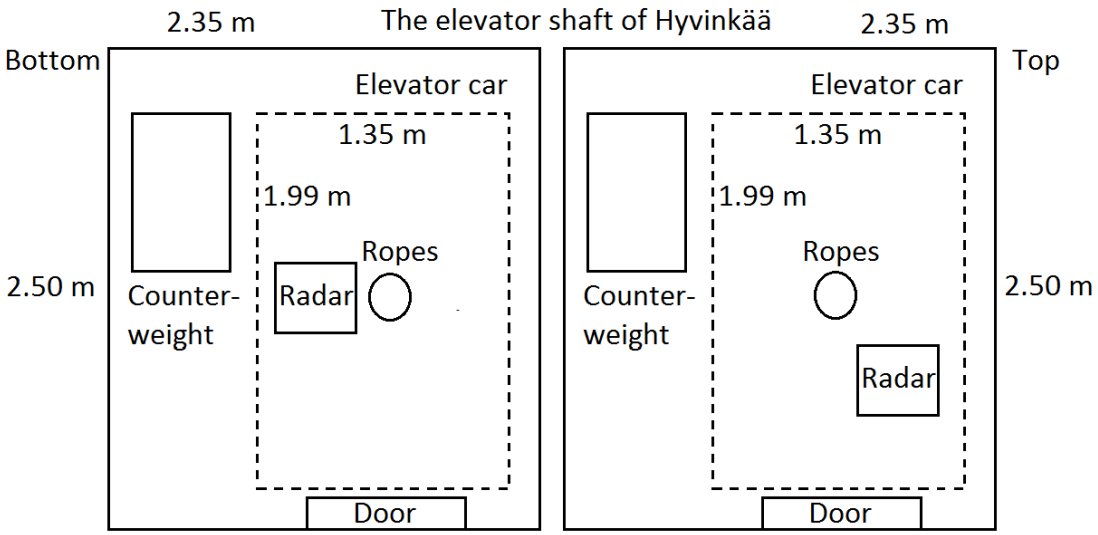

Figure 19: A cross-section of radar placement in the elevator shaft of Hyvinkää. The placement used in the measurement setup towards the bottom of the car is on the left side and the placement in the measurement setup towards the ceiling is on the right side of the figure.

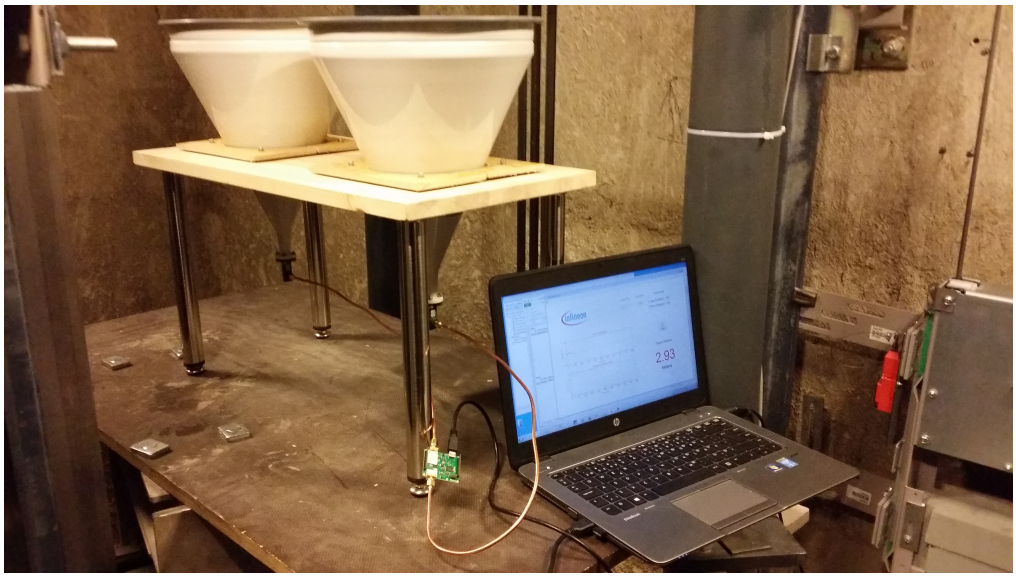

Figure 20: Sense2Go2 module set for measuring towards the bottom of the elevator car in the shaft of Hyvinkää.

The physical appearance of the bottoms of elevator cars depends on the used elevator. This might cause differences from signal reflection between different elevator cars. The elevator cars used in the tests have reflective surfaces at many height levels as seen in Figure 26. This might cause several echo signal peaks close to each other and thus affect the measurement results.

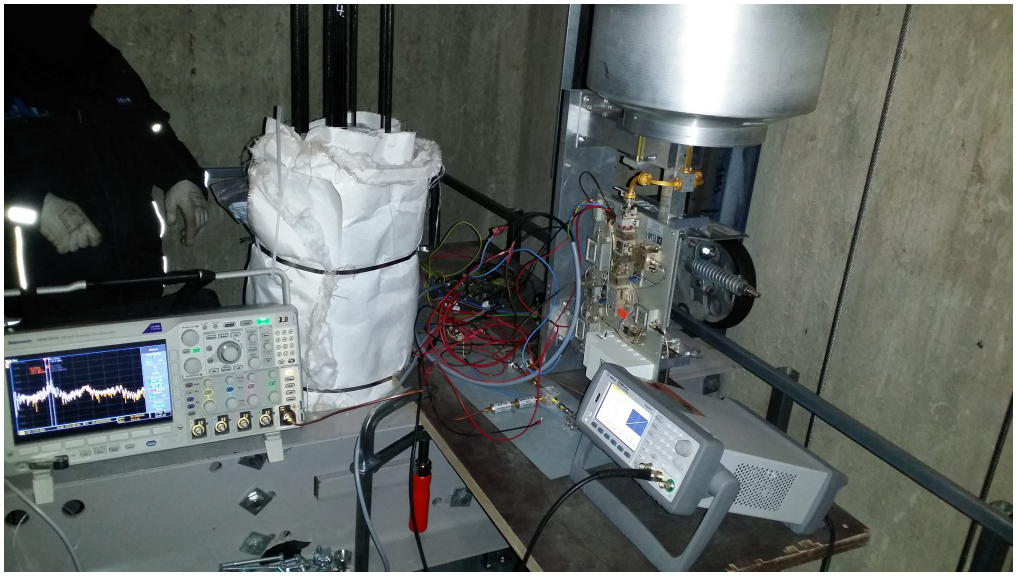

Figure 21: Elva-1 measuring towards the ceiling of the shaft in the elevator shaft of Hyvinkää.

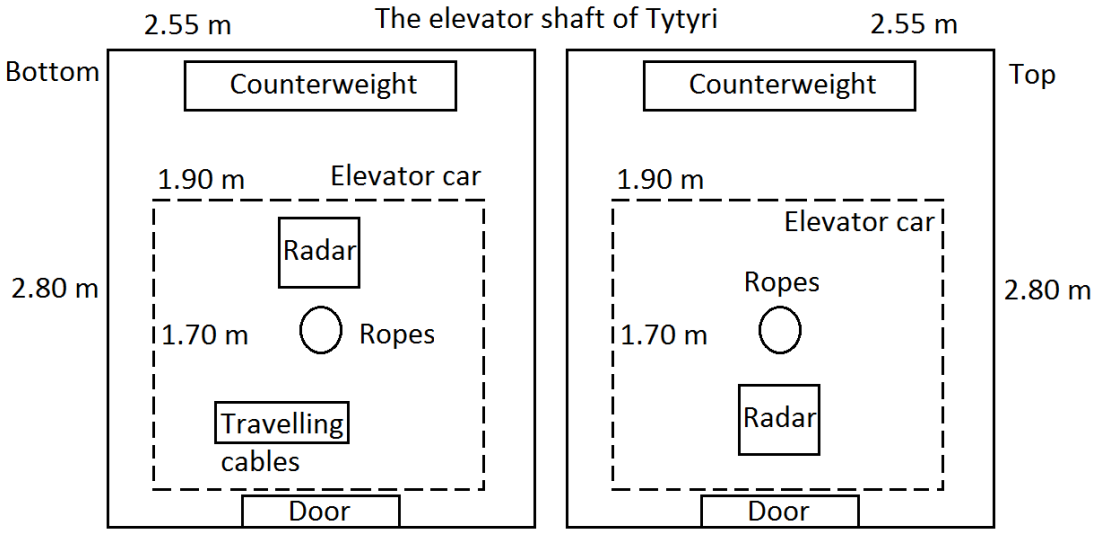

Figure 22: A cross-section of radar placement in the elevator shaft of Tytyri. The placement used in the measurement setup towards the bottom of the car is on the left side and the placement in the measurement setup towards the ceiling is on the right side of the figure.

Figure 23: Elva-1 measuring towards the bottom of the elevator car in the elevator shaft of Tytyri.

Figure 24: SiversIMA radar module measuring towards the bottom of the elevator car in the elevator shaft of Tytyri. Ten meter D9 cable connects the laptop to the power controller board. The long cable enables radar control outside of the shaft.

Figure 25: Measurement setups towards the ceiling of the elevator shaft of Tytyri. On the left side of the figure is 77 GHz radar and on the right side is 60 GHz radar. Radars are inside the spoiler, which reduces air drag. The top piece of the spoiler has been removed for transmitting and receiving signals. This 50 cm hole is seen in the middle of figure.

Figure 26: Bottom of the elevator car in Hyvinkää is presented on the left and the bottom of the car in Tytyri is on the right side of the figure. The radar corner reflector is attached to the bottom of the elevator car of Tytyri.

4.2 Concrete structure shaft

The test site at Hyvinkää is presented in Figure 27. Walls of the shaft are made of concrete and the ceiling consists of several horizontal metal plates. Dimensions of the shaft are 2.35 m * 2.50 m, which gives the reflecting surface of the ceiling as 5.88 m^2.

The longest hoistway is 50 meters and the maximum speed of the elevator is 6 [m/s]. The test elevator is equipped with light ropes, whose load bearing member is made of carbon fiber composite and, thus, are lighter than steel ropes. Concentrating on electromagnetic properties, light rope reflects radar signals less than steel rope. The signal attenuation is larger with light rope, which may reduce the radar range. Nevertheless, the hoistway is probably not long enough for this phenomenon to appear. Signal attenuation by light rope reduces possible interfering reflections caused by ropes.

Figure 27: The concrete elevator shaft of Hyvinkää. Light ropes and the metallic ceiling of the shaft are seen in the figure.

In the concrete elevator shaft of Hyvinkää, the measurement points according to the elevator height reference are presented in Table 7. These points are floors and are used for practical reasons to guarantee exactly the same measurement point intervals between different radars. Stopping accuracy of an elevator car on floors is ±3 millimeters [1]. Possible changes to shaft properties caused by the different elevator locations are kept in minimum by using floors as measurement points.

4.3 Steel structure shaft

Tytyri mine is located in Lohja and it is the tallest elevator test facility in the world. This KONE High-rise laboratory is the only shaft in the world, where elevators with speeds up to 17.0 [m/s] may be tested. There are two elevators in the

Table 7: Measurement heights at concrete elevator shaft of Hyvinkää.

Floor	**Lift height reference [m]**
1	0
2	2.90
3	5.85
4	8.75
5	11.65
6	14.56
7	17.48
8	26.25
9	35.00
10	43.75
11	48.29

shaft and the longest hoistway in Tytyri is 333 meters. The normal temperature is close to +6 Celcius degrees with dripping water and high humidity. These are tough circumstances and elevators passing tests in these extreme conditions likely withstand any condition that a modern building might face.

The shaft of Tytyri is made of steel and it is presented in Figure 28. The ceiling of the shaft consists of horizontal metal plates and thus it is similar to the ceiling of the elevator well in Hyvinkää in Figure 27. The dimensions of the shaft are 2.55 m * 2.80 m, which sets the maximum reflecting surface area to 7.14 m^2. The ropes of the test elevator are made of steel. Steel ropes might increase the radar range due to reflections. However, increased reflections cause also increased radar signal scattering.

High rise elevators sometimes have spoilers at a bottom and at a top of an elevator car for air drag and noise reduction. Nevertheless, these spoilers turn the radar signal to the walls and disturb the measurements greatly or make the fastening of the measurement equipment difficult. At the bottom of the elevator car, the spoiler is disconnected during the measurements. The top piece of the spoiler is removed at the top of the elevator car, which makes a 50 cm hole for radar operation. The hole is seen in Figure 25 with measurement setups on top of the elevator car.

In the steel shaft of Tytyri, the stationary measurements are made with an interval of ten meters. Between the measurement points, the elevator car is moved in maintenance mode and the control system of the elevator is used as a height reference. Stopping an elevator car with high accuracy location tuning between the floors in maintenance mode is time consuming and not the greatest concern about these measurements. Hence the elevator car is stopped as close to the intervals of 10 meters as possible while keeping the measuring fluent. This causes small variations to elevator location between different measurements. Changes in elevator locations are within ±20 cm and in most cases the difference is only a couple of centimeters. Every elevator location is monitored by the accuracy of 1 cm.

Figure 28: The steel shaft and ropes of Tytyri.

A moving elevator is tested in the shaft of Tytyri. Six different situations are tested, which are acceleration, decelaration and the elevator driving at maximum speed. These three situations are tested both the elevator car approaching the radar and the elevator car leaving from radar. The elevator car has an acceleration of 1 m/s^2 and a maximum speed of 10 m/s.

4.4 Safety

Scientific research into possible health effects has been unable to keep pace with the rapid qrowth of radio frequency (RF) and microwave frequency (MW) devices and applications in our working and living environment. Health is defined as the state of complete physical, mental and social well-being and not the absence of disease or infirmity by World Health Organization (WHO). [50]

The known effect of RF and MW exposure is tissue heating. [51] Temperature rises in tissue exceeding 1 Celsius degree above their normal temperature can lead to adverse biological effects. Thermal hazards are thought to exist only above thresholds [50].

Low intensity, non-thermal RF/MW radiation has not been considered having biological effects although numerous scientific reports suggest such effects. Biological effects possibly associated with RF/MW radiation are childhood leukemia, brain tumours, genotoxic effects, neurological effects and neurodegenerative diseases, immune system deregulation, allergic and inflammatory responses, breast cancer, miscarriage and some cardiovascular effects. Prolonged exposures may reasonably be presumed to lead in these health effects. Though no known health hazards caused by non-thermal radiation are scientifically proven [50, 52]. Nevertheless, potential biological effects from low level RF exposure need further research [50]. [53]

RF and MW safety standards are made for protecting human health. The

most commonly used standards in the whole world are based on the IEEE C95 standards, the recommendations of the National Council on Radiation Protection and Measurements (NCRP), and the guidelines of the International Commission on Non-Ionizing Radiation Protection (ICNIRP) and the International Radiation Protection Association (IRPA). [52]

The maximum permissible exposure levels of the IEEE standard C95.1a-2005 at different frequencies are presented in Table 8. Slight differences between the exposure limits at RF/MW frequencies exist between countries and they are related to engineering interpretations and applied safety factors - the not disagreement of the biological effects of the radiation [52]. For instance, Australian Radiation Protection and Nuclear Safety Agency (ARPANSA) has slightly different averaging times than IEEE standard, nevertheless, the exposure limits are equal [54]. The human body size at different ages is illustrated in Table 9 for better understanding about the radiation exposure limits.

Table 8: The maximum permissible exposure levels of the IEEE standard C95.1a-2005 for general public. In controlled environments, more severe radiation is accepted. Averaging time is the time period over which exposure is averaged. f is the frequency in GHz. [55]

Frequency range (GHz)	**RMS power density (W/m^2)**	**Averaging time (min)**
0.4 - 2	$0.001f/200$	30
2 - 5	10	30
5 - 30	10	$150/f$
30 - 100	10	$25.24/f^{0.476}$
100 - 300	$(90f - 7000)/200$	$5048/[(9f - 700)f^{0.476}]$

Table 9: Reference values for human body size at different ages. [56]

	Height (cm)		**Mass (kg)**		**Surface area (m^2)**	
Age	**Male**	**Female**	**Male**	**Female**	**Male**	**Female**
Newborn	51	51	3.5	3.5	0.24	0.24
1 year	76	76	10	10	0.48	0.48
5 years	109	109	19	19	0.78	0.78
10 years	138	138	32	32	1.12	1.12
15 years	167	161	56	53	1.62	1.55
Adult	176	163	73	60	1.90	1.66

In the scope of this thesis, 24 GHz, 60 GHz and 77 GHz are the most interesting frequency areas. Continuous radio frequency and microwave radiation with intensity less than 10 W/m^2 are improbable to affect physiology through athermal mechanisms

[57]. The total power dissipation of the Infineon radar module is 750 mW, the transmitter power of Elva-1 is 10 mW and the power consumption of Sivers IMA is 3 W. All of these radars are well below the radiation exposure limits. In addition, the elevator shaft is a restricted area for public people. Thick walls of the shaft attenuate the penetrating radiation, which is already within acceptable limits. Therefore, the elevator shaft is a safe place for placing radar. RF exposure for ordinary people is possible only when the elevator door is open and then the exposure time is only a couple of seconds. Maintenance people may get exposure to radiation, but the levels are well below the standard limits. Thus, safety is on the adequate level in this application.

5 Results

Chapter 5 introduces the calculation methods used achieving the range data and the measurement results in different environments. In the following figures 36, 38, 43 and 45 showing the measurement results measured towards the shaft ceiling, the actual distance is inverted due to measuring from the top of the elevator car. An elevator height reference being maximum, the distance from radar to the shaft ceiling is at minimum.

Distance to the target is calculated by Equation 16. The refractive index, n, for neutral air is used as 1.0003 in calculations [22]. Radar frequency sweep bandwidth, Δf_t, is dependable on used radar. Echo signal frequency, Δf_e, is measured straigth in the elevator shaft or calculated from the measurements.

A correct sweep time of radar, t_s, is crucial for Equation 16. Sweep times depend on the ideality of the signal generator and the SiversIMA's radar module. Different sweep times than the correct one produce a linear error to the calculated range results compared with the real elevator car location as seen in Figure 29. Even 1 ms error in the sweep time affects much to the calculated distance, which makes error compensation important.

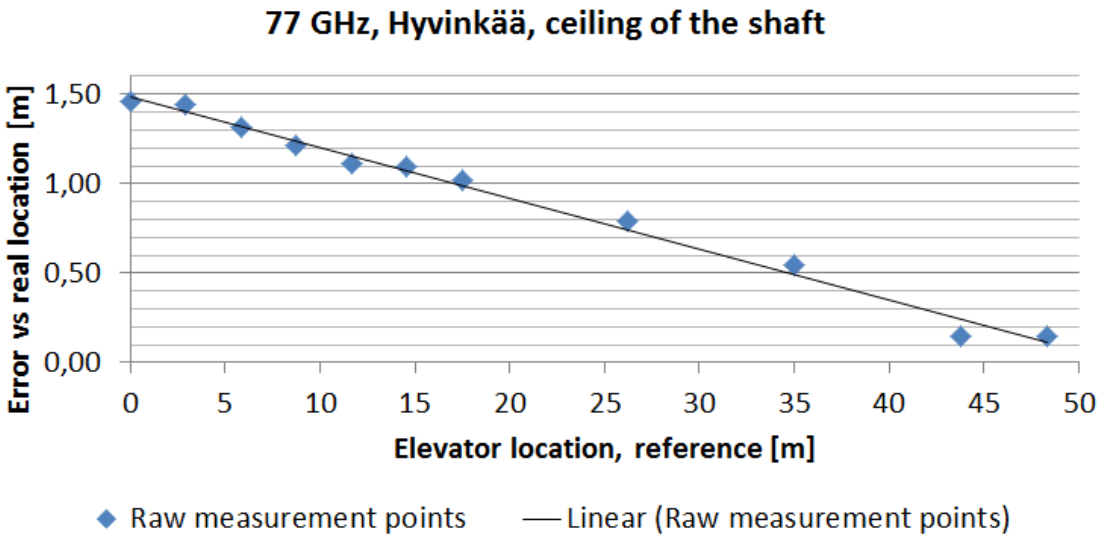

Figure 29: Uncompensated measurement results of 77 GHz radar at the shaft of Hyvinkää. Measurements are done towards the shaft ceiling. A trend line is drawn to the results.

The error can be compensated by drawing a graph similar of Figure 29. The calculated range point errors are compared with the real locations, which are achieved from the elevator height reference system. This error is growing well linearly along the distance to the target. The next step is to draw a trend line and set its slope on zero by setting the sweep time correctly. The slope of the ascending trend line is set on zero by correcting the sweep time, t_s, with equation

$$t_s = -k_{tr} t_s + t_s, \tag{23}$$

where k_{tr} is the slope of the trend line. For descending trend line the compensation equation is given by

$$t_s = k_{tr} t_s + t_s. \tag{24}$$

This numerical iteration reduces the sweep time error each time Equation 23 or 24 is used. The trend line direction of the original graph defines whether to use Equation 23 or 24 during the whole compensation process. In the situation of Figure 29, Equation 24 should be used during the compensation. Sweep time is compensated with the accuracy of 10^{-6} seconds in the results presented in sections 5.2 and 5.3. Some of this existing linear error may also be caused by reflections from the shaft walls and ropes. Nevertheless it is a minority part of the error since testing outside of the elevator shaft the radar distance is compensated correctly with Equations 23 and 24.

A systematic measurement error is also present, which results from the radar distance to the elevator car bottom or to the ceiling of the shaft. For instance, an elevator car at height 0 meters gives the radar range of a couple of meters when measuring to the bottom of the elevator car. This error can also be compensated with the previous drawn trend line by setting the zero slope trend line to go along with the x-axis. The compensated results of Figure 29 are presented in Figure 43. The slope of the trend line is set to zero by accuracy of 10^{-5} in Figures 35-38 and 42-45. The calculated sweep times are presented along the results.

5.1 Infineon Technologies 24 GHz

Sense2Go2 radar module faced operational problems. Range results acquired by the software were not close to real distances and they regularly swung. The block diagram of Figure 8 shows that the received signal faces a low noise amplifier (LNA) first. Right after LNA raw signal IFIL can be measured with an oscilloscope. This raw signal is presented in Figure 30 with the tuning voltages of the local oscillator V_{coarse} and V_{fine}, where the gain of the LNA is set on its minimum value. The IFIL signal is cut, which is definitely one factor for the software not being accurate with the range information.

The adjustable gain of the LNA is set to 10 as default. Adjustment gain range is from 5 to 1000. The gain is set to 5 by removing the resistor R135. Though the raw signal data does not improve significantly. The antennas of Figure 10 are quite large and close to each other, which can lead to the malfunction of the LNA. Therefore the raw signal is checked without connecting the receiving antenna at all, but the cutting does not decrease with this setup.

Operation of the receiver and the transmitter is researched with the setup of the block diagram of Figure 31. The test arrangements in practice are shown in Figure 32. The raw signal IFIL is measured with oscilloscope when a synthesized sweeper is feeding the receiving antenna connector. The operation of the module and transmission of signals are confirmed with a spectrum analyzer connected to the

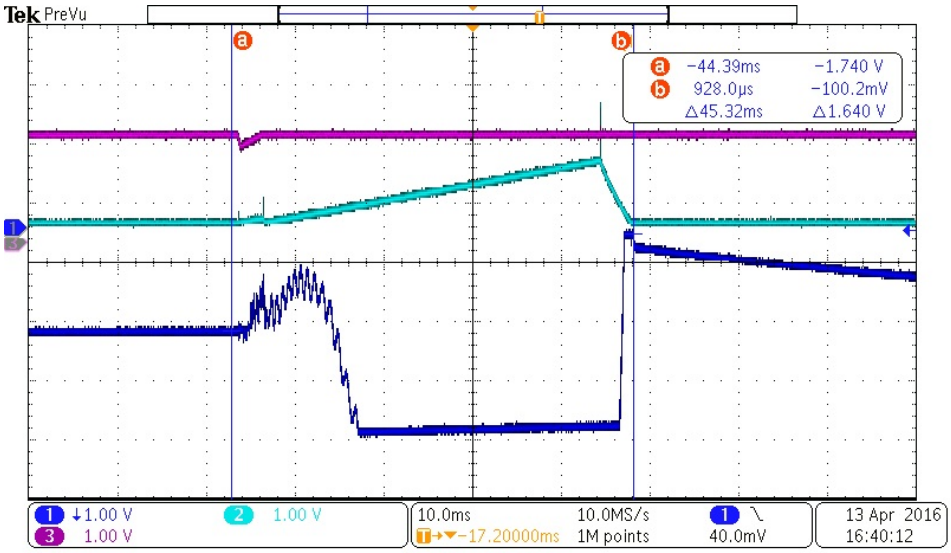

Figure 30: Raw signal data $IFIL$ presented with dark blue, V_{coarse} with cyan and V_{fine} with pink. Gain of the LNA is set to minimum.

antenna. Different echo signal effects on the raw signal data are simulated with the synthesized sweeper. Unfortunately, the IFIL does not respond to any changes made by the sweeper. The data remains the same, whether the signal is generated to the receiver or not.

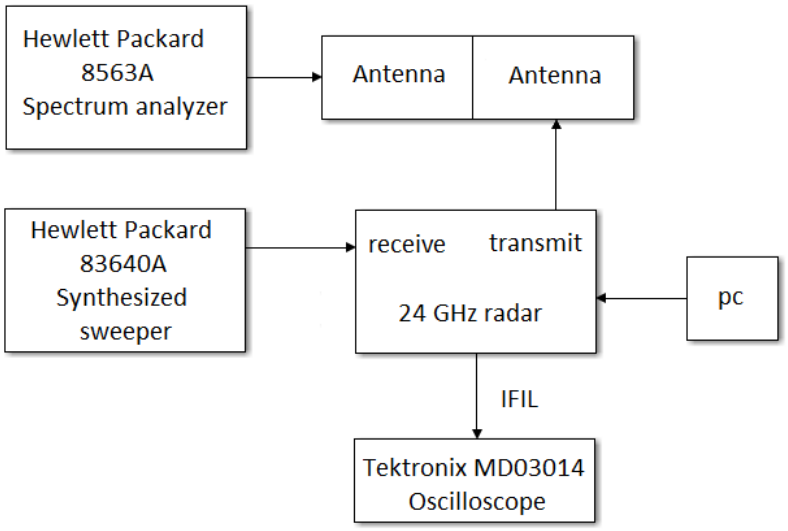

Figure 31: Block diagram of the receiver measurements.

The malfunction of the module may have been caused when modifying the PCB for antenna connectors. No operational tests were done during the modifying process of the subcontractor. FMCW mode and the software for the FMCW operation of the Sense2Go2 module were also in a preliminary stage in the module. Infineon

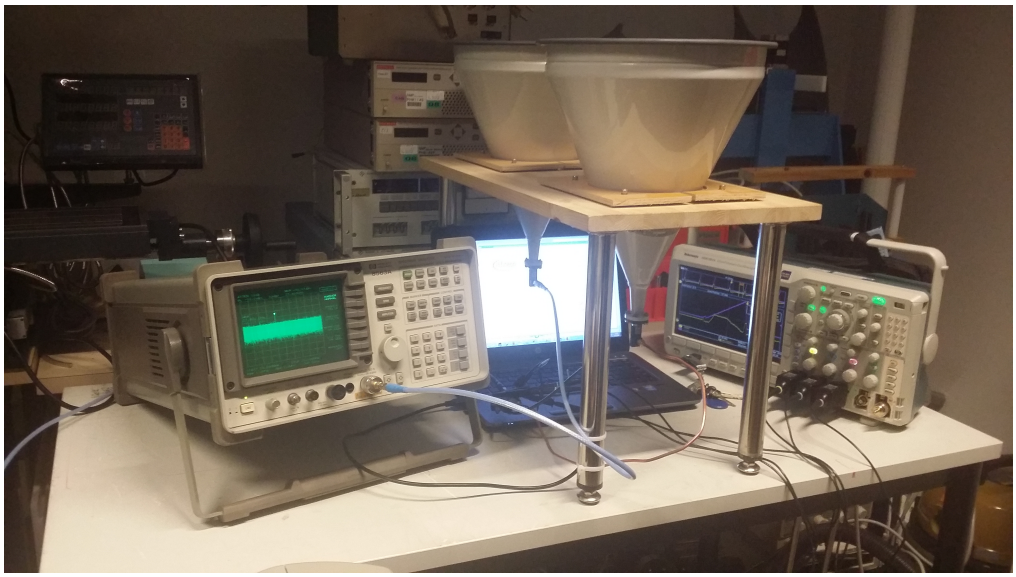

Figure 32: Measurement setup of the block diagram of Figure 26.

Technologies does not market the module for distance measurements anymore. Nevertheless, the module was not capable of measuring distances to the elevator due to the occasions of this chapter.

5.2 Elva-1 60 GHz

The original FFT spectrum of Elva-1 is checked with a measurement towards the sky. The spectrum is presented in Figure 33. Figure 34 presents one example of the spectrum in the steel shaft of Tytyri.

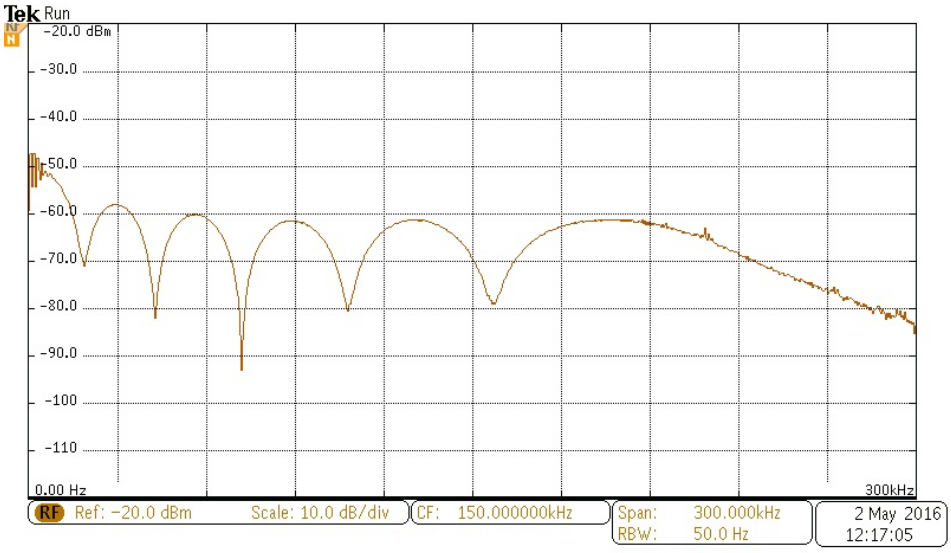

Figure 33: FFT spectrum of Elva-1 measured towards the sky.

Some oscillation is seen in Figure 33 up to 200 kHz. This results from the test setup of Figure 14. The waveform produced by the signal generator may have small oscillation or the voltage controlled oscillator can not hold single frequency points ideally and thus it is swinging. Nevertheless the oscillation seen in Figure 33 is not a problem for the measurements due to the small amplitude.

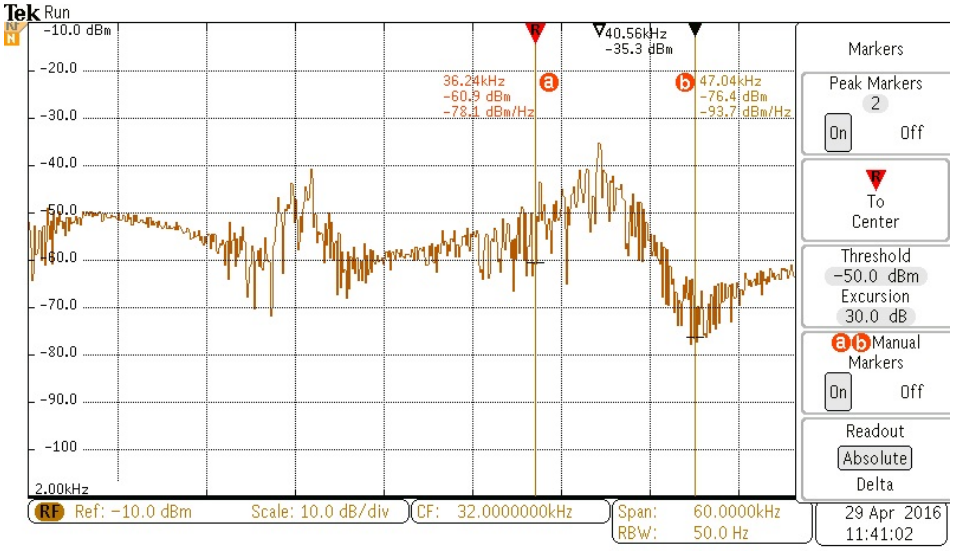

Figure 34: An example of FFT spectrum of Elva-1 in the elevator shaft of Tytyri.

The target echo frequency, Δf_e, is measured straigth with the oscilloscope. Time of the frequency sweep, t_s, is calculated by Equation 22. The frequency is set by the signal generator of Figure 14. The sweep bandwidth, Δf_t, is 376.81 MHz as presented in section 3.2. Range information can be acquired by Equation 16 and the error compensation process is described at the beginning of Chapter 5.

The range results compared with the elevator height reference are presented in Figures 35-38. Results of the concrete shaft of Hyvinkää are showed in Figures 35 and 36. Results of the steel shaft of Tytyri are presented in Figures 37 and 38. The measured range is inverted in Figures 36 and 38 due to measuring from the top of the elevator car.

The results achieved by different radars are comparable in stationary situations and thus the basis for the movement detection is achievable by both radars. Measuring a moving elevator car with the setup of Elva-1 is challenging. Access to the shaft is forbidden while the elevator is moving in normal mode due to safety reasons. The test setup of 60 GHz radar demands the manual control of the oscilloscope and thus catching and analyzing all the peak frequencies is difficult in real time. Some video camera arrangements for the screen of the oscilloscope could be made, but measuring with 77 GHz radar is more practical. Though the moving elevator spectrum is checked more precisely only with 77 GHz radar. With 60 GHz radar, changing radar echo FFT spectrum is seen on the screen of the oscilloscope while the elevator car is moving.

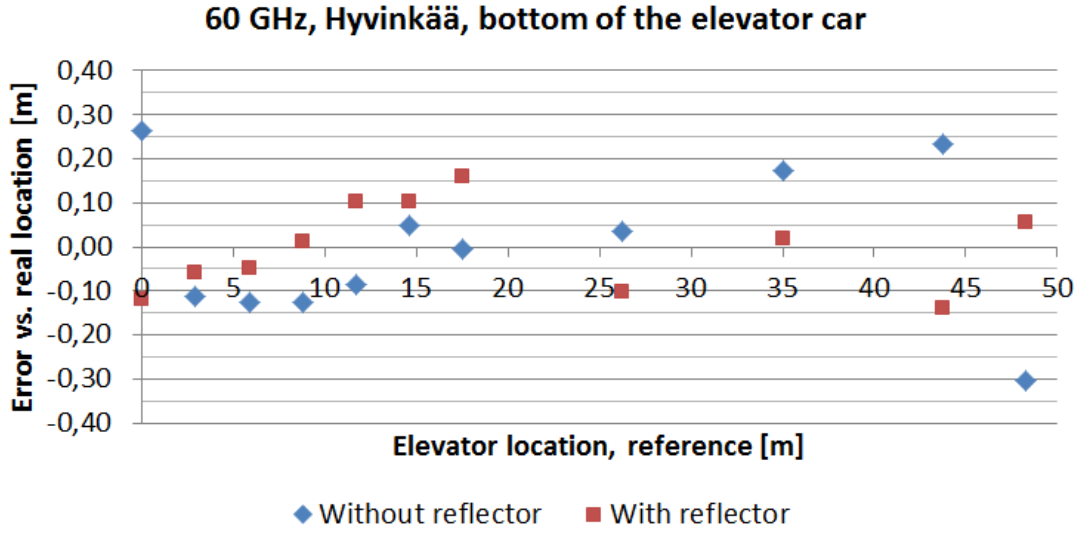

Figure 35: The measurement results of 60 GHz radar measured to the bottom of the elevator car without a radar corner reflector in the concrete structure shaft in Hyvinkää. The sweep time was thought as 10 ms though after correction it is 9.303 ms.

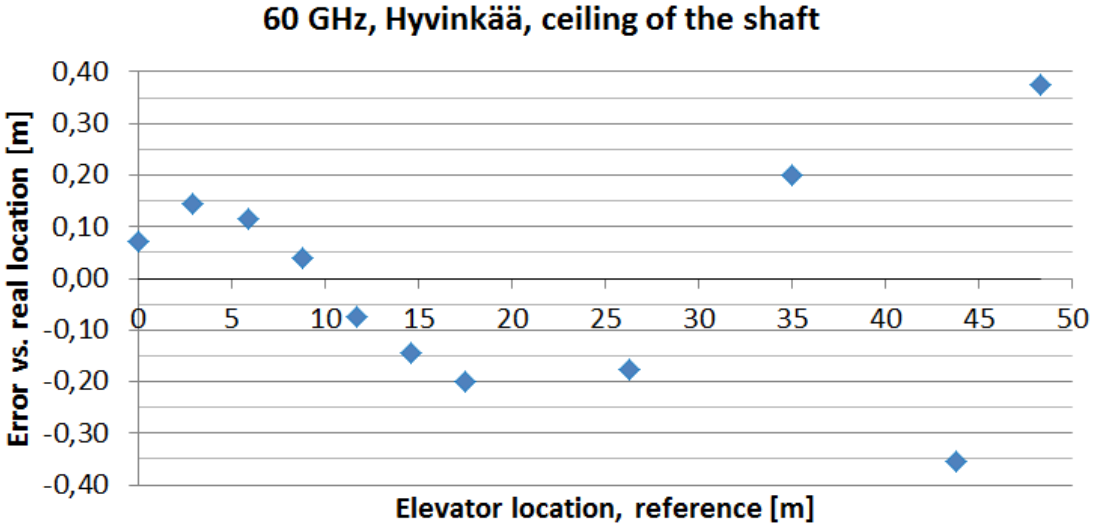

Figure 36: Elva-1 measurement results measured to the ceiling of the shaft without radar corner reflector in concrete structure shaft in Hyvinkää. The sweep time was thought as 10 ms though after correction it is 9.358 ms.

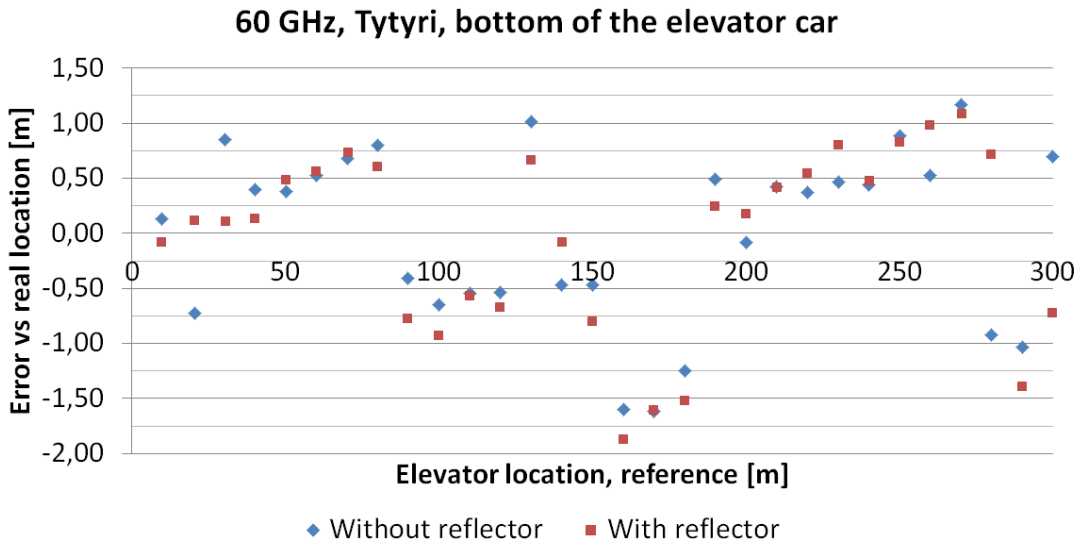

Figure 37: Elva-1 measurement results measured to the bottom of the elevator car without radar corner reflector in steel structure shaft in Tytyri. The sweep time was thought as 10 ms though after correction it is 9.695 ms.

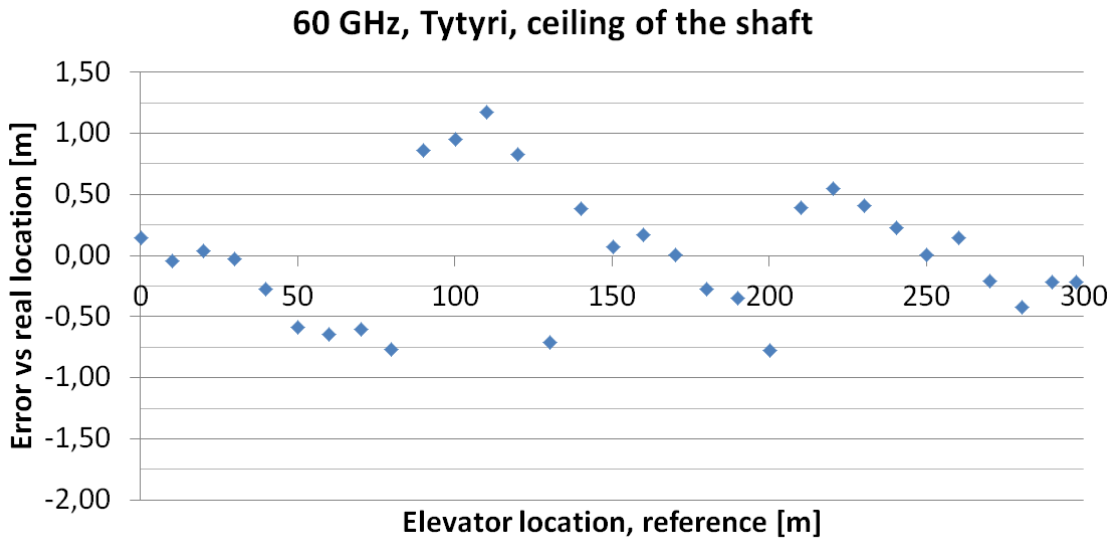

Figure 38: Elva-1 measurement results measured to the ceiling of the shaft without radar corner reflector in steel structure shaft in Tytyri. The sweep time was thought as 10 ms though after correction it is 9.707 ms.

5.3 Sivers IMA 77 GHz

Radar performance is checked towards the sky, in other words, there are no targets to detect. The raw data measured towards the sky is presented in Figure 39. A low frequency component is seen in the results. The maximum level of output IF signal is approximately 500 mVpp and signal components with this magnitude may exist in typical measurements due to inadvertent reflections in the system, even though it is unlikely [49]. For comparison, the raw signal data in the concrete shaft of Hyvinkää is shown in Figure 40. A Fourier transform has to be performed for the raw data to get the target echo frequency, Δf_e. The FFT and echo peak searching are done with Matlab software. An example of the FFT spectrum in an elevator shaft is shown in Figure 41.

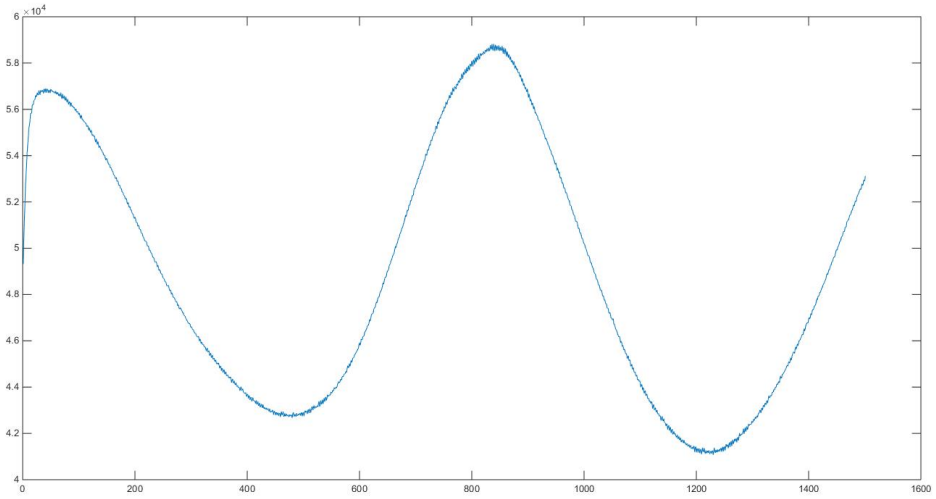

Figure 39: The raw signal data of the RS3400W/04 measured towards the sky.

Range results compared with the elevator height reference system are presented in Figures 42-45. Results of the concrete shaft of Hyvinkää are shown in Figure 42 and 43, and the results of the steel shaft of Tytyri in Figures 44 and 45. The maximum bandwidth of 1.5 GHz is used in the measurements of Hyvinkää.

Measurements towards the shaft ceiling are made with the radar corner reflector connected 2.7 m below the ceiling in Hyvinkää. This 2.7-meter distance between the shaft ceiling and the corner reflector should produce separate peaks in the measurements. Although the echo peaks of the reflector are weak in comparison with the peaks of the ceiling. This difference is seen in the FFT spectrum of Figure 41. In addition, the reflector is not visible in every measurement. For these reasons the corner reflector is not used and further researched in the measurements towards the shaft ceiling.

Range resolution and maximum unambiguous range need to be taken into account in the shaft of Tytyri. Equation 19 sets the maximum range at 75 m with $\Delta f_t = 1.5$ GHz. The highest calculated bandwidth for achieving 300 meter range is 374.9 MHz.

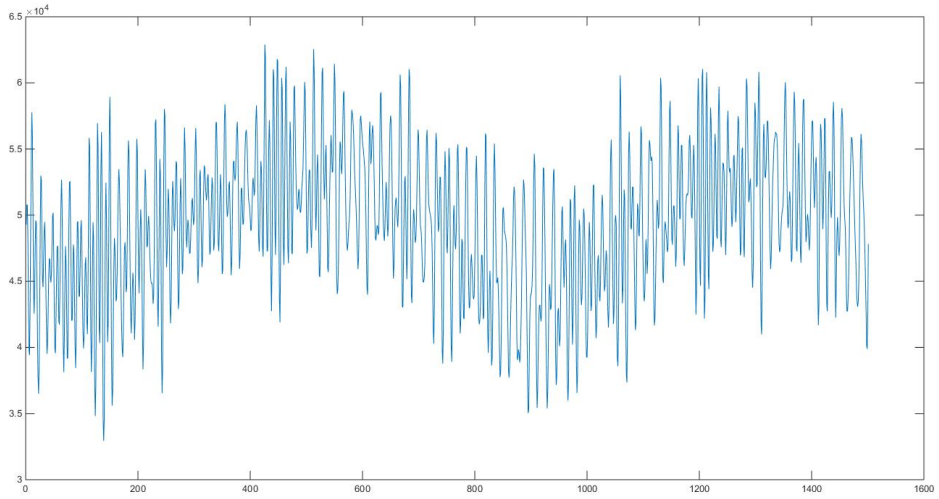

Figure 40: Raw signal data measured in the elevator shaft floor 10 of Hyvinkää towards the shaft ceiling with the radar corner reflector.

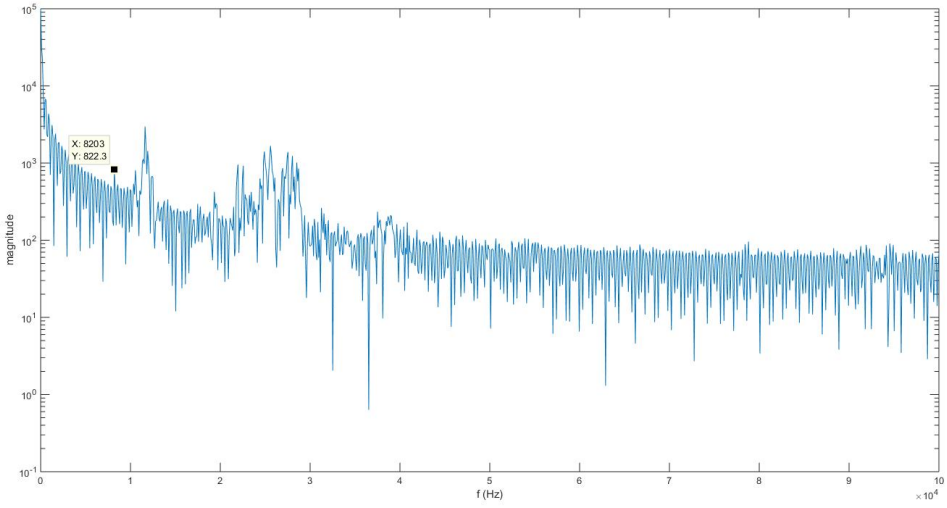

Figure 41: FFT performed for the raw signal data. The data is measured in the elevator shaft floor 10 of Hyvinkää towards the shaft ceiling with the radar corner reflector. The shaft ceiling produces echo at 11.6 kHz and the corner reflector 2.7 m below at 8.2 kHz.

Elva-1 has the bandwidth of 376.81 MHz and for comparison the same bandwidth is used also in 77 GHz radar. In Figures 42 and 43, the range results are presented with two different radar signal bandwidths. The bandwidth of 376.81 MHz is used for the whole shaft length and the maximum bandwidth of 1.5 GHz for the first 75-meter distances.

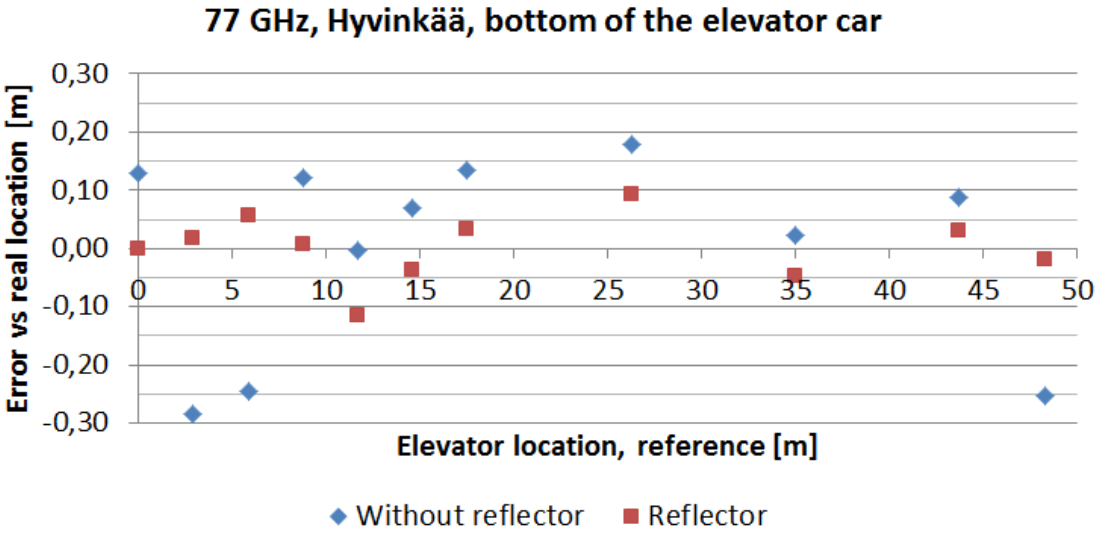

Figure 42: Sivers IMA measurement results measured to the bottom of the elevator car with and without radar corner reflector in concrete structure shaft in Hyvinkää. The sweep time was thought as 75 ms though after correction it is 72.853 ms.

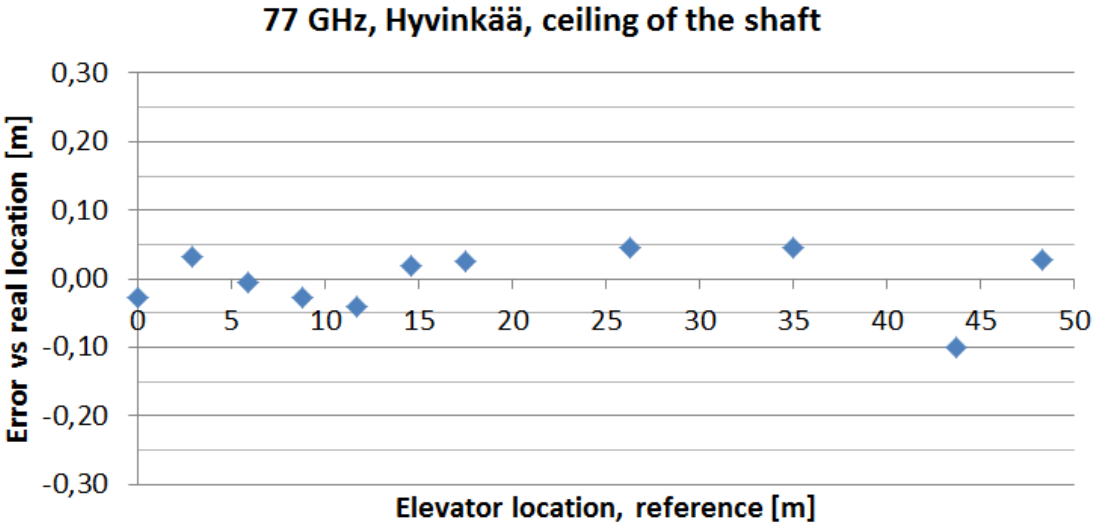

Figure 43: Sivers IMA measurement results measured to the ceiling of the shaft without radar corner reflector in concrete structure shaft in Hyvinkää. The sweep time was thought as 75 ms though after correction it is 72.927 ms.

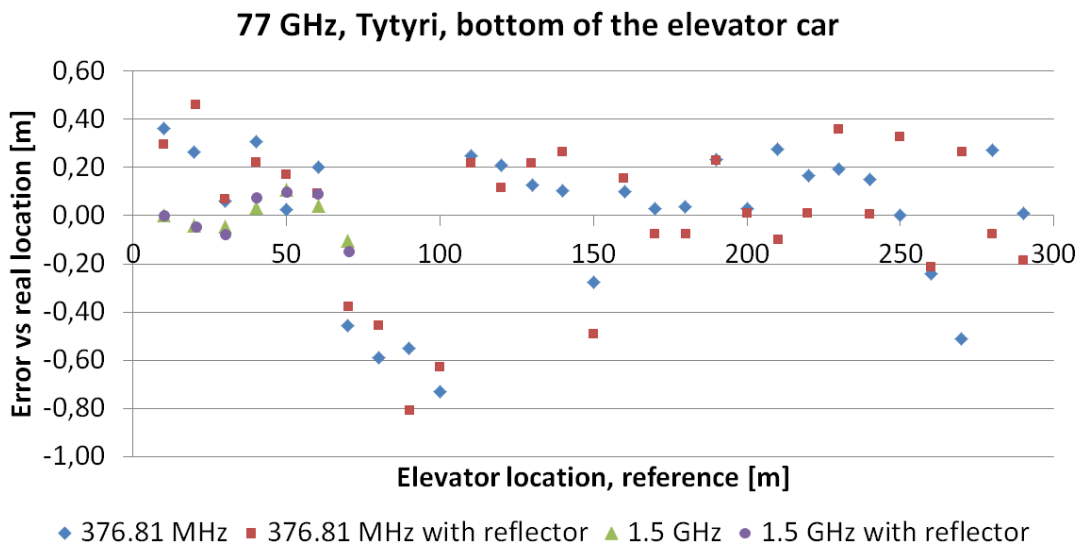

Figure 44: Sivers IMA measurement results measured to the bottom of the elevator car with and without radar corner reflector in steel structure shaft in Tytyri. The results are presented with two different bandwiths. The sweep time was thought as 75 ms though after correction for 1.5 GHz bandwidth it is 75.108 ms and for 376.81 MHz bandwidth it is 75.044 ms.

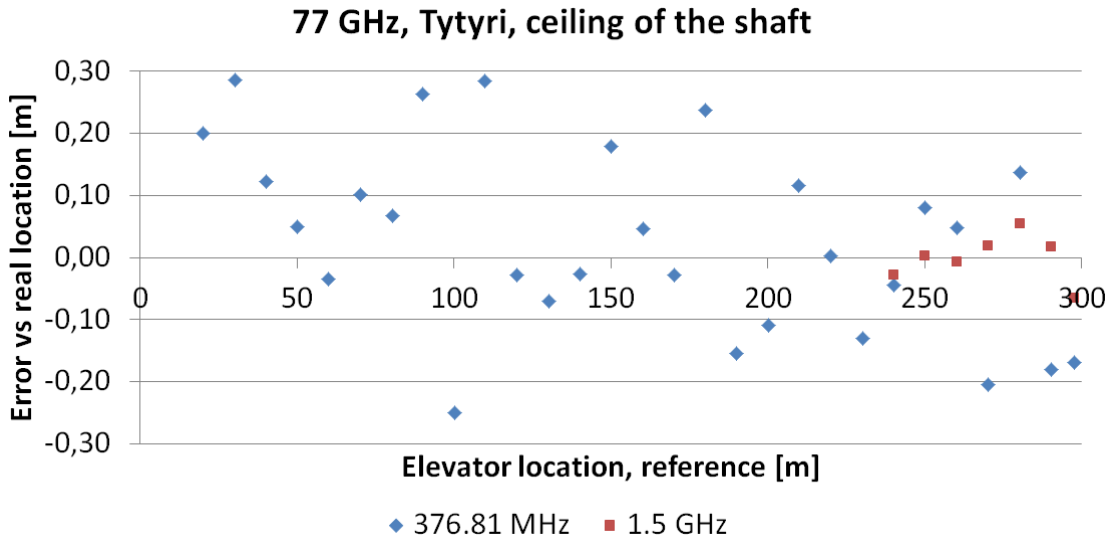

Figure 45: Sivers IMA measurement results measured to the ceiling of the shaft without radar corner reflector in steel structure shaft in Tytyri. The sweep time was thought as 75 ms though after correction for 1.5 GHz bandwidth it is 74.956 ms and for 376.81 MHz bandwidth it is 75.165 ms.

An FFT spectrum of an accelerating elevator car is shown in Figure 46. The elevator is moving away from radar. The echo peak is slightly wider than in stationary cases, but still very clear to read. Used signal bandwidth was 1.5 GHz. An elevator at the speed of 10 meters per second was measured with the bandwidth of 376.81 MHz. The FFT spectrum is presented in Figure 47. The elevator should be seen between 50 kHz and 70 kHz, but no clear peak is detected. The results were the same, whether the elevator was approaching the radar or moving away from radar. Also decelerating situation on the other side of the shaft produced no detectable results, but decelerating elevator near the radar was measurable as good as in Figure 46.

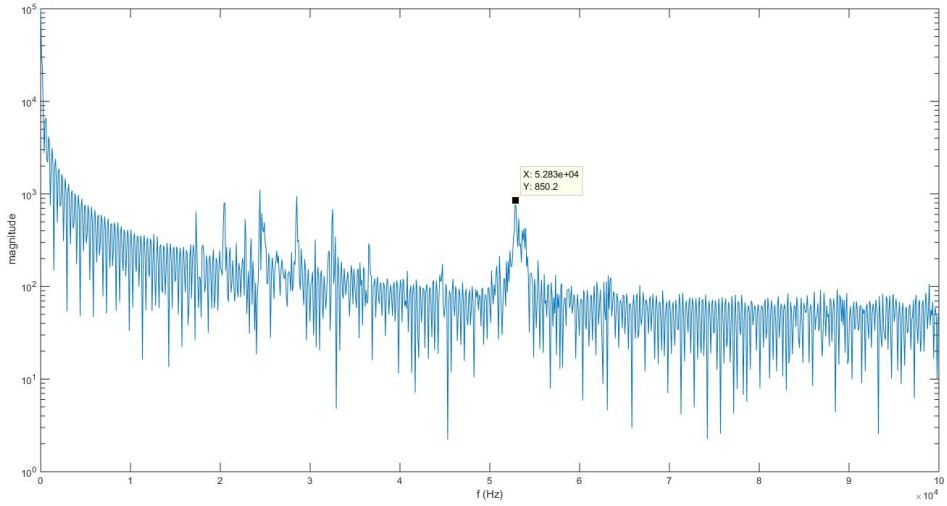

Figure 46: An FFT spectrum of an accelerating elevator in the shaft of Tytyri. The speed of the elevator is 5 meters per second and it is seen at 52.8 kHz.

5.4 Discussion

This section discusses about the achieved results and occasions behind them.

5.4.1 Theory vs practice

According to the range resolution theory and Equation 7, acquired results with 77 GHz radar are really good within the range resolution limits in all test cases. Only a couple of measurement points exceed the accuracy of the theory of 40 cm in the measurements towards the bottom of the car in Tytyri. With 60 GHz radar, the theory is also accurate in the shaft of Hyvinkää. The measured results are not within the 40 cm range resolution in the shaft of Tytyri, but are not exceeded much. These results of a stationary elevator car indicate the elevator well being a suitable environment for radar measurements.

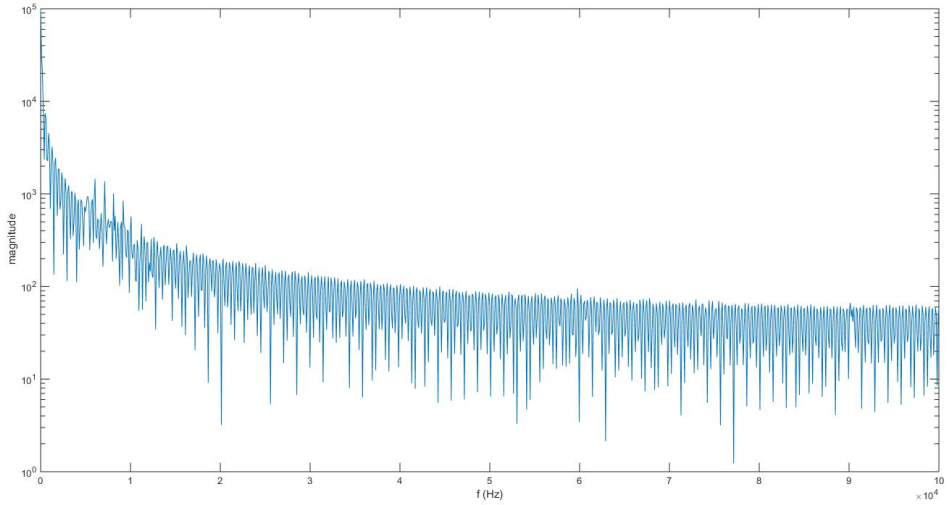

Figure 47: An FFT spectrum of the elevator at the speed of 10 meters per second. Elevator location should be seen between 50 kHz and 70 kHz.

The range resolution theory affects much radar accuracy, which is seen in Figures 44 and 45. The same measurement points with various transmitted signal bandwidths give clearly better results with the higher resolution.

The maximum range by Equation 19 have to take into account in the shaft of Tytyri. With 77 GHz radar, the transmitted signal bandwidth have to be reduced for most of the measurements in Tytyri. Ranges more than calculated maximums by Equation 19 are not visible at all with 77 GHz radar since the echo spectrum is not wide enough for the echo peak to be visible. The maximum measurable range in the elevator shaft is close to calculated ones. Though reflections from walls and ropes do not increase or decrease the maximum range significantly.

5.4.2 Attenuation of signal

Signal attenuation is seen with both radars when measuring to a bottom of a car. Attenuation becomes notable at over 200 m distances, when measuring to the bottom of the car. With 60 GHz radar, the echo peaks are usually within 5 dBm after 170 m distances. According to Figure 2, the attenuation at 60 GHz is three to four decibels at the distance of 200 meters. A radar signal has to travel to the elevator car and back to radar, which makes the attenuation a significant factor. A radio wave absorbed over ten decibels by oxygen is possible at 60 GHz at the other end of the shaft. The FFT spectrums become more open to interpretations than in short distances and though interpretation errors are possible. One example of interpretation is presented in Figure 48. Knowledge of the place where the elevator car should be is vital for the interpretation in some situations. The graph of Figure 2 gives an attenuation of 0.5 dB/km at 77 GHz. With 77 GHz radar, the attenuation seems to affect less and interpretation is needed only at over 200 m distances. Though in most cases the

correct peaks are quite easily readable.

When measuring towards the shaft ceiling, the attenuation does not seem as strong as in the bottom measurement setup. The FFT spectrums are somewhat clearer, which probably results from the really good reflective surface of the ceiling. In Figures 36, 38, 43 and 45, better accuracy is seen than in the corresponding bottom measurements in Figures 35, 37, 42 and 44. Hence, measuring from the top of the elevator car seems to be preferable.

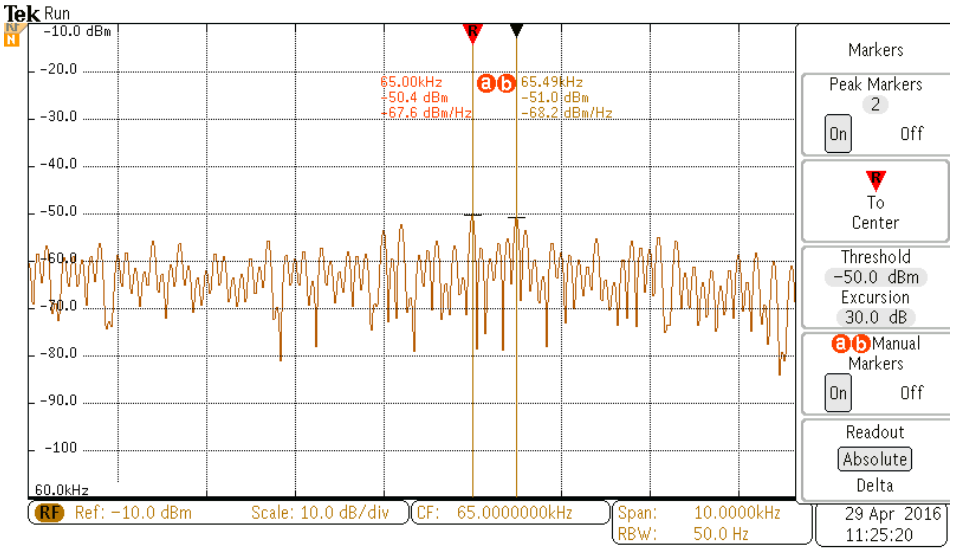

Figure 48: An example of attenuation of 60 GHz signals. The FFT spectrum is measured towards the ceiling of Tytyri's shaft. Distance to the ceiling is 250 meters (65 kHz).

5.4.3 Reflection of signal

A bottom of an elevator car has usually reflecting metal surfaces at many height levels as presented in Figure 26. This occasionally causes several echo signal peaks close to each other. 77 GHz radar has maximum range resolution of 10 cm, which supports seeing more than one peak in the FFT spectrum at the elevator car location. Though, these extra peaks are usually not so powerful and thus, do not cause problems reading the spectrums of 77 GHz radar. With 60 GHz radar, this phenomenon is seen slightly more, even though the range resolution is 40 cm. Especially in Tytyri at longer distances the phenomenon is notable and sometimes interpretation is needed, when the powers of the peaks are close to each other. The majority of the measurements to the bottom of the car are still clearly readable.

The radar corner reflector does not reflect signals as well as the shaft ceiling made of horizontal metal plates. The difference of reflection is seen in the FFT spectrum of Figure 41 and in the results of bottom measurements compared with the results of the ceiling measurements. In Figure 41, the reflector is 2.7 m below the ceiling. Both produce own echo peaks, but the magnitude of the reflector peak at 8.2 kHz is

well below the peak of the ceiling at 11.6 kHz. Nevertheless, the advantage of the reflector is seen when measuring to the bottom of the elevator car. In Figures 35, 37, 42 and 44, show that with the reflector slightly better accuracy is achieved. Hence, the corner reflector is an asset when the reflective surface is not as excellent as the shaft ceilings of Hyvinkää and Tytyri.

A moving counterweight is occasionally seen in the FFT spectrums. Though it is not visible in all possible situations. Significant differences in counterweight existence are seen in FFT spectrums depending on the radar placement. For instance, the measurement setup closer to the counterweight in Tytyri produces the most and the strongest echoes of counterweights in all test cases. Placing radar on the other side of ropes as in the top setup in Figure 22 reduces the magnitude of the counterweight echoes significantly and detecting them in all possible situations is not unambiguous as in the bottom setup in Figure 22. In the shaft of Hyvinkää, the counterweight is not clearly seen in either the setups of Figure 19. In some of the FFT spectrums of Hyvinkää, the counterweight is recognizable though not as clearly as in measurements at Tytyri. Overall the counterweight existence in FFT spectrums did not disturb or cause harms to measuring. An elevator car induces greatly stronger echoes when the car and counterweight are close to each other.

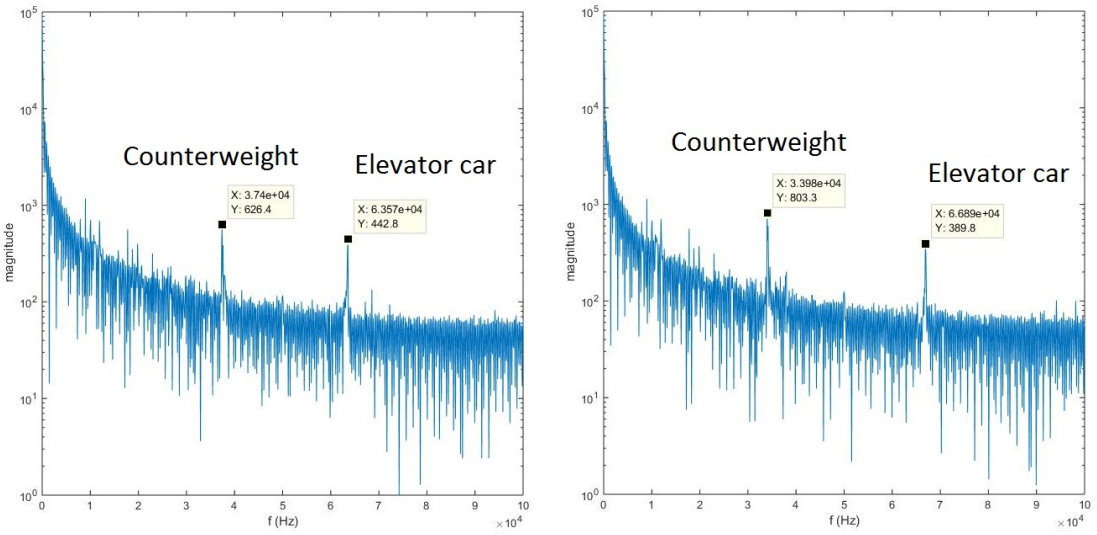

Figure 49: The figure presents two consecutive FFT spectrums measured towards the bottom of the elevator car in Tytyri. Distances to the car are 190 m (63.57 kHz) and 200 m (66.89 kHz) whereas distances to the counterweight are 100 m (33.98 kHz) and 110 m (37.40 kHz).

An elevator car produces similar FFT spectrums whether it is in move or in place. However, echo peaks of the spectrums in moving situations are slightly wider than in stationary cases. This results from the measurement speed of the radar module. During the sweep time of 75 milliseconds the elevator moves tens of centimeters depending on the speed. In the case of Figure 46, the elevator has moved 37.5 centimeters during the measurement, which is probably the main reason for a slightly

wider echo seen at 52.8 kHz.

5.4.4 Conclusions and future research

If the measuring is done towards the ceiling of the shaft, changes are required to the spoiler, which reduces air drag and noise. A hole needs to be left for signal transmission or the measuring devices have to be connected outside the spoiler, which is definitely not a good thing for the air drag reduction. Probably the best compromise between the signal transmission and the air drag reduction is connecting the antenna(s) to the top of the spoiler and tightening other measuring devices inside the spoiler. Then only an antenna would be added to the shape of the spoiler and no additional holes are required. Effects of the connected radar on air drag should be investigated.

The results show that 77 GHz radar of SiversIMA is more accurate and thus has more potential than 60 GHz Elva-1 radar for continuous monitoring of the elevator car speed and location. However the single sweep time of SiversIMA radar is not sufficient for fulfilling the desired minimum criteria of 20 measurements per second. The sweep time of 75 ms indicates possible performance around 10 to 13 measurements per second with optimized software. With Elva-1 the sweep time can be set high enough and the oscillator can be changed to one with wider frequency range for achieving higher transmitted signal bandwidths. Although the accuracy of Elva-1 could have been better with the studied combination compared with the theory. Signal attenuation of 60 GHz radar in an elevator shaft is too much for accurate and unambigious radar system. Thus, inspection of new parts for 60 GHz radar does not generate as much interest as continuing with 77 GHz radar. Nevertheless, the sweep time of radar should be below 50 ms in order to the system having enough time for signal processing and calculations. The results of 77 GHz radar look encouraging for the continuous ETSL system if the measurement speed of radar could be modified higher.

A moving elevator seems to be measurable by radars and it should be researched more specifically. The single spectrums of the moving elevator car look promising for continuous elevator speed and location monitoring as long as the distance is less than 75 meters. When the maximum range of 77 GHz radar is increased from 75 meters by reducing the transmitted signal bandwidth, radar is not capable of detecting the elevator car moving 10 meters per second. Attenuation should not be a problem at these 10 meters per second measurements due to the stationary FFT spectrums are clear and have strong echo peaks at these distances. The operating principle of radar is based on a phase change in a frequency sweep, which is produced by single discrete step frequencies. [49] The phase measurement is triggered at each step frequency. During one frequency step (50 μs), the elevator moves 0.5 mm. This movement is large in comparison with the wavelength (3.9 mm) of the carrier wave. An unambiguous phase difference does not exist because of this and thus radar is not capable of detecting the moving elevator car at the speed of 10 meters per second. FMCW radars with a linear frequency sweep would be able to measure moving elevator cars. Movement causes doppler frequencies, which produce measurement

errors but would not destroy the whole measurement.

To conclude the thesis, an elevator shaft is a suitable environment for radar measurements and 77 GHz FMCW radar has potential to replace the present speed and location measurement tools in the ETSL system. Though studied radars can not replace the present speed and location measuring system directly. The future challenges are software development and radar modifications. Software is needed for radar automatic control and calculation processes for radars studied in this thesis. The inspected 77 GHz radar module needs improvements in sweep time to be fast enough for the ETSL system.

6 Summary

In this thesis, radar applicability for elevator speed and location measurement was evaluated. The evaluation was done by measuring with the selected radar modules both in steel and concrete elevator shafts. Measuring was done towards the bottoms of elevator cars as well as towards the ceilings of the shafts. The operation principles as well as advantages and disadvantages of various radar technologies were discussed. Based on these findings, 24 GHz, 60 GHz and 77 GHz FMCW radars were chosen for tests on elevator shafts. Two of the radar modules were commercially available and the third one, Elva-1, required additions to the FMCW operation.

The best accuracy of stationary location measurements was achieved by 77 GHz radar. Its accuracy was within range resolution theory in all measurements done towards the ceilings of the shafts and only a few exceeds of theory limits in measurements towards the bottoms of the elevator cars. Hence, the ceilings of the shafts were discovered to be better reflectors than the bottoms of the elevator cars. A radar corner reflector was also studied in the thesis. Its effects remained low in the measurements towards the ceilings due to ceiling being such a good reflector itself. Though the radar corner reflector showed to have a positive effect on the results when measuring towards the bottoms of elevators.

The speed and location measurement of an elevator at the speed of 10 meters per second was not observable. The elevator accelerating to this speed was clearly measurable, but after achieving the speed of 10 meters per second the elevator escaped from the inspected radar.

The goal of this thesis was to evaluate the feasibility of employing radar for measuring elevator speed and location and propose radar for the ETLS system. An elevator shaft was discovered to be a suitable environment for radar measurements. However, the studied radar modules were not directly suitable for the ETSL system due to a too slow measurement rate. As a replacement of the current ETSL system, 77 GHz radar of Sivers IMA is promising whether its sweep time could be modified to faster. Other suggestions are finding another commercial 77 GHz FMCW radar or developing a one.

Further research is especially needed about the situations where an elevator car is moving although the studied radars need modifications before that. The radar transponder system was not researched in this thesis due to low commercial availability. Situation should be kept in the picture. Also that technology has possibilities - at least on paper.

References

[1] KONE Corporation. *KONE Minispace 1.6 With KDH Drive Technology Book*. Hyvinkää, 2005.

[2] *NEN-EN 81-20 Safety rules for the construction and installation of lifts - Lifts for the transport of persons and goods - Part 20: Passenger and goods passenger lifts*, NEN-EN Standard 81-20, 2011.

[3] Infineon Technologies AG, Sense2Go2 Description. http://www.infineon.com/dgdl/Infineon-PB_Sense2Go_Development_Kit-PB-v02_00-EN.pdf?fileId=5546d4624b0b249c014bbb516b23395d. Accessed: 2016-01-04.

[4] Sivers IMA, Datasheet of RS3400W/04 module. http://siversima.com/wp-content/uploads/RS3400W04_DataSheet.pdf. Accessed: 2016-01-21.

[5] Elva-1, designing and manufacturing company's website. http://elva-1.com/. Accessed: 2016-06-28.

[6] Jukka Ruoskanen. Tools and methods for radar performance evaluation and enchancement. Doctoral Dissertation, Helsinki University of Technology, 2005.

[7] Merril I. Skolnik. An introduction and overwiev of radar. In Merril I. Skolnik, editor, *Radar Handbook*. McGraw-Hill, the United States of America, 2008.

[8] Richard G. Curry. *Radar essentials: A Concise Handbook for Radar Design and Performance Analysis*. Raleigh, NC: SciTech Pub., 2011.

[9] David K. Barton. *Radar System Analysis and Modeling*. Artech House Inc., Norwood, 2005.

[10] Bin-Feng Lin, Yi-Ming Chan, Li-Chen Fu, Pei-Yung Hsiao, Li-An Chuang, Shin-Shinh Huang, and Min-Fang Lo. Integrating appearance and edge features for sedan vehicle detection in the blind-spot area. *Intelligent Transportation Systems, IEEE Transactions on*, 13(2):737–747, 2012.

[11] David K. Barton. *Radars Volume 2: The Radar Equation*. Artech House Inc., Massachusetts, 1977.

[12] David K. Barton. *Radars Volume 7: CW and Doppler Radar*. Artech House Inc., Massachusetts, 1980.

[13] Merril I. Skolnik. *Introduction to Radar Systems*. McGraw-Hill, Singapore, 2001.

[14] Ministry of Internal Affairs and Communcations, table of radio frequency allocations of Japan, 2015-05. http://www.tele.soumu.go.jp/resource/e/search/myuse/use0303/10g.pdf. Accessed: 2016-04-12.

[15] The European table of frequency allocations and applications in the frequency range 8.3 kHz to 3000 GHz, 2015-05. http://www.erodocdb.dk/docs/doc98/official/pdf/ERCRep025.pdf. Accessed: 2016-04-12.

[16] Table of frequency allocations of Federal Communications Commission, 2016-03-04. https://transition.fcc.gov/oet/spectrum/table/fcctable.pdf. Accessed: 2016-04-12.

[17] Table of radio frequency allocations of the Republic of China, 2005-12-19. http://www.ncc.gov.tw/english/files/07060/92_070605_1.pdf. Accessed: 2016-04-12.

[18] Mohinder Jankiraman. *Design of multi-frequency CW radars*. SciTech Publishing, the United States of America, 2007.

[19] KB Cooper, RJ Dengler, G Chattopadhyay, E Schlecht, J Gill, A Skalare, I Mehdi, and PH Siegel. A high-resolution imaging radar at 580 ghz. *Microwave and Wireless Components Letters, IEEE*, 18(1):64–66, 2008.

[20] Eugene F. Knott, John F. Shaeffer, and Michael T. Tuley. *Radar Cross Section*. Artech House Inc., Dedham, 1985.

[21] K. G. Budden. *The Propagation of Radio Waves: The Theory of Radio Waves of Low Power in the Ionosphere and Magnetosphere*. Cambridge University Press, Great Britain, 1985.

[22] Wayne L. Patterson. The propagation factor, F_p, in the radar equation. In Merril I. Skolnik, editor, *Radar Handbook*. McGraw-Hill, the United States of America, 2008.

[23] Kevin R Petty and William P Mahoney III. Weather applications and products enabled through vehicle infrastructure integration (vii) feasibility and concept development study. Technical report, 2007.

[24] Simon Haykin and Michael Moher. *Modern Wireless Communications*. Pearson Education Inc., the USA, 2005.

[25] Elodie Richalot, Matthieu Bonilla, Man-Fai Wong, Victor Fouad-Hanna, Henri Baudrand, and Joe Wiart. Electromagnetic propagation into reinforced-concrete walls. *Microwave Theory and Techniques, IEEE Transactions on*, 48(3):357–366, 2000.

[26] John D. Kraus and Ronald J. Marhefka. *Antennas For All Applications*. McGraw-Hill, Singapore, 2003.

[27] Antti Räisänen and Arto Lehto. *Radiotekniikan perusteet*. Otatieto, Helsinki, 2001.

[28] SSi Cable Corporation, table of coaxial cable properties. http://www.ssicable.com/images/stories/ssi/Cable_Selection_combined2.pdf. Accessed: 2016-04-27.

[29] HUBER+SUHNER, microwave cable catalog. http://literature.hubersuhner.com/Technologies/Radiofrequency/MicrowavecabelesEN/?page=93. Accessed: 2016-06-28.

[30] Radar tutorial physical fundamentals of the radar principle. http://www.radartutorial.eu/01.basics/pic/radarprinzip.print.jpg. Accessed: 2016-01-20.

[31] Olli Klemola and Arto Lehto. *Tutkatekniikka*. Otatieto, Helsinki, 1998.

[32] William W. Shrader and Vilhelm Gregers-Hansen. MTI radar. In Merril I. Skolnik, editor, *Radar Handbook*. McGraw-Hill, the United States of America, 2008.

[33] Michael R. Ducoff and Byron W. Tietjen. Pulse compression radar. In Merril I. Skolnik, editor, *Radar Handbook*. McGraw-Hill, the United States of America, 2008.

[34] Sven Roehr, Peter Gulden, and Martin Vossiek. Precise distance and velocity measurement for real time locating in multipath environments using a frequency-modulated continuous-wave secondary radar approach. *Microwave Theory and Techniques, IEEE Transactions on*, 56(10):2329–2339, 2008.

[35] Dean D. Howard. Tracking radar. In Merril I. Skolnik, editor, *Radar Handbook*. McGraw-Hill, the United States of America, 2008.

[36] Roger Sullivan. Synthetic aperture radar. In Merril I. Skolnik, editor, *Radar Handbook*. McGraw-Hill, the United States of America, 2008.

[37] Andrew G Stove. Linear fmcw radar techniques. In *IEE Proceedings F (Radar and Signal Processing)*, volume 139, pages 343–350. IET, 1992.

[38] HD Griffiths. New ideas in fm radar. *Electronics & Communication Engineering Journal*, 2(5):185–194, 1990.

[39] Wikipedia continuous wave radar. https://en.wikipedia.org/wiki/Continuous-wave_radar#/media/File:Fmcw_prinziple.png. Accessed: 2016-01-20.

[40] Ilari Hänninen, Mikko Pitkonen, Keijo Nikoskinen, Jukka Sarvas, et al. Method of moments analysis of the backscattering properties of a corrugated trihedral corner reflector. *Antennas and Propagation, IEEE Transactions on*, 54(4):1167–1173, 2006.

[41] Kamal Sarabandi and Tsen-Chieh Chiu. Optimum corner reflectors for calibration of imaging radars. *Antennas and Propagation, IEEE Transactions on*, 44(10):1348–1361, 1996.

[42] Xia Ye, H Kaufmann, and XF Guo. Landslide monitoring in the three gorges area using d-insar and corner reflectors. *Photogrammetric Engineering & Remote Sensing*, 70(10):1167–1172, 2004.

[43] KM Keen. New technique for the evaluation of the scattering cross-sections of radar corner reflectors. In *IEE Proceedings H (Microwaves, Optics and Antennas)*, volume 130, pages 322–326. IET, 1983.

[44] John N. Briggs. *Target Detection By Marine Radar*. The Institution of Electrical Engineers, United Kingdom, 2004.

[45] Zeno W Wicks Jr, Frank N Jones, S Peter Pappas, and Douglas A Wicks. *Organic coatings: science and technology*. John Wiley & Sons, 2007.

[46] Ismo Lindell. *Aaltojohtoteoria*. Otatieto, Helsinki, 1997.

[47] Mario A Maury Jr. Microwave coaxial connector technology: a continuing evolution. *Maury Microwave Corporation*, pages 1–21, 2005.

[48] Paul Pino. Intermateability of sma, 3.5 mm and 2.92 mm connectors-examination of the history and motivation behind sma, 3.5 mm and 2.92 mm connectors in an effort to determine their mechanical intermateability. *Microwave Journal; International ed*, 10:18, 2007.

[49] Sivers IMA, FMCW radar application note. http://siversima.com/wp-content/uploads/FMCW-Radar-App-Note.pdf. Accessed: 2016-05-24.

[50] Michael H Repacholi. Low-level exposure to radiofrequency electromagnetic fields: Health effects and research needs. *Bioelectromagnetics*, 19(1):1–19, 1998.

[51] Anders Ahlbom, Adele Green, Leeka Kheifets, David Savitz, and Anthony Swerdlow. Epidemiology of health effects of radiofrequency exposure. *Environmental health perspectives*, pages 1741–1754, 2004.

[52] Eleanor R Adair and Ronald C Petersen. Biological effects of radiofrequency/microwave radiation. *Microwave Theory and Techniques, IEEE Transactions on*, 50(3):953–962, 2002.

[53] Lennart Hardell and Cindy Sage. Biological effects from electromagnetic field exposure and public exposure standards. *Biomedicine & Pharmacotherapy*, 62(2):104–109, 2008.

[54] *Maximum Exposure Levels to Radiofrequency Fields - 3 kHz to 300 GHz*, ARPANSA, Radiation Protection Series No. 3, 2002.

[55] J.C. Lin. A new ieee standard for safety levels with respect to human exposure to radio-frequency radiation. *Antennas and Propagation Magazine, IEEE*, 48(1):157–159, 2006.

[56] Jack Valentin. Basic anatomical and physiological data for use in radiological protection: reference values: Icrp publication 89. *Annals of the ICRP*, 32(3):1–277, 2002.

[57] Robert K Adair. Biophysical limits on athermal effects of rf and microwave radiation. *Bioelectromagnetics*, 24(1):39–48, 2003.